Cancer-Targeting Multifunctionalized Gold Nanoparticles in Imaging and Therapy

P.F. Jiao[1], H.Y. Zhou[2], L.X. Chen[3] and B. Yan*[,2,4]

[1]*School of Pharmaceutical Sciences, Shandong University, Jinan, Shandong, 250012, China*

[2]*Department of Chemical Biology and Therapeutics, St. Jude Children's Research Hospital, Memphis, TN, 38105, USA*

[3]*Yantai Institute of Coastal Zone Research, Chinese Academy of Sciences, Yantai, Shandong, 264003, China*

[4]*School of Chemistry and Chemical Engineering, Shandong University, Jinan, Shandong, 250100, China*

Abstract: Nanotechnology has provided many promising nanoplatforms for targeted cancer imaging and therapy. Among these platforms, gold nanoparticles (GNPs) play a unique role in medicine because of their excellent physical and chemical properties. To expand the applications of GNPs in medicine, amounts of targeting moieties, imaging labels, and therapeutic agents have been integrated into these particles to form multifunctionalized GNPs. In this review, we highlight recent advances of the fabrication of cancer-targeting multifunctionalized GNPs and their applications in imaging and therapy.

Keywords: Gold nanoparticles, targeting moieties, therapeutic payloads, conjugation methods, cancer imaging, cancer therapy.

1. INTRODUCTION

To treat cancer, an effective drug must not only kill tumor cells, but also be soluble in water in order to travel through the bloodstream, evade the immune system to avoid being cleared out by the liver or kidneys, and find its targets. Traditional small-molecule drugs have to incorporate all these functions into single molecules.

Nanomedicine employs nanoparticles as imaging probes and therapeutic agents to treat cancer and other human disorders [1]. Unlike traditional medicines, nanomedicine can be artificially engineered to optimize multiple functions and combine different components into a single nanostructure. Nanoparticle surfaces can be tailored for solubility, friendliness to immune cells, and target-seeking ability, while the particles' drug cargoes can also be built to kill tumor cells [2]. For decades, nanoplatforms such as liposome, polymer, protein-bound particles, gold nanoparticles (GNPs), superparamagnetic iron oxides, and quantum dots have been developed for imaging and therapy of cancers (Fig. **1**) [3-8]. Of these, "proof of concept" has been provided for GNPs for diagnosis and therapy of various types of cancers, and thus GNPs present realistic potential for clinical translation [9]. Their unique physical and chemical properties include biocompatibility, size- and shape-dependent optical and electronic features, and readily modifiable surfaces [10].

GNPs can target tumors passively or actively (Fig. **2**). Passive targeting uses the unique properties of the tumor microenvironment, especially (1) the leaky tumor vasculature, which is more permeable than normal tissue to macromolecules, and (2) a dysfunctional lymphatic drainage system, which increases retention of macromolecules in the tumor tissue [13-17]. These effects generate enhanced permeability and retention (EPR), which allows GNPs to extravasate through these gaps into extravascular spaces and accumulate inside tumor tissues [18]. The biggest limitation of passive tumor targeting is the inability to achieve a sufficiently high level of nanoparticle concentration at the tumor site, resulting in low therapeutic and imaging efficacy and eliciting undesirable systemic adverse effects [16]. In the EPR effect, although poor lymphatic drainage helps enrichment of extravasated nanoparticles in the tumor interstitium, it also induces nanoparticles' outflow from the tumor as a result of elevated osmotic pressure in the interstitium, which eventually leads to their redistribution in some portions of the cancer tissue [18, 19]. To overcome these limitations, the alternative strategy of conjugating the targeting moieties such as tumor-homing peptides, aptamers, or antibodies to GNPs to obtain targeted GNPs can be used. Many active targeting strategies, in fact, use the EPR effect so that active and passive targeting mechanisms act synergistically in many of the targeted delivery systems [16].

*Address correspondence to this author at the School of Chemistry and Chemical Engineering, Shandong University, Jinan, Shandong, 250100, China and Department of Chemical Biology and Therapeutics, St. Jude Children's Research Hospital, Memphis, TN, 38105, USA; E-mail: Dr.bingyan@gmail.com

2. MULTIFUNCTIONALIZED GOLD NANOPARITLCES (GNPS)

Multifunctionalized GNPs are composed of GNPs surrounded by targeting moieties; therapeutic payloads; and hydrophilic polymer coatings such as polyethylene glycol (PEG), polysaccharides, poloxamines, or poloxamers. As these platforms are compatible with X-rays, they have been developed as radiotherapy enhancement agents and computed tomography (CT) imaging contrast agents.

2.1. GNPs

On the basis of their shapes and physical properties, GNPs are divided into several subtypes (Fig. **3**). The earliest studied GNPs were gold nanospheres; subsequently, gold nanorods and nanocages were reported. The most popular method to synthesize GNPs is by chemical reduction of gold salts such as hydrogen tetrachloroaurate ($HAuCl_4$) using citrate as the reducing and stabilizing agent [21]. This method produces monodisperse spherical GNPs of diameters 10-20 nm. However, production of larger GNPs (40-120 nm) by this method offers low yields, often resulting in polydisperse particles. Brown and Natan reported a seeding approach for the synthesis of monodisperse GNPs of diameters 30-100 nm [22]. This method uses the surface of GNPs as a catalyst for the hydroxylamine-driven reduction of Au^{3+}. Subsequently, Murphy and colleagues employed this seed-mediated growth approach to control the shape and size of the nanoparticles [23, 24]. Borohydride-reduced GNPs seeds (3-4 nm in diameter) were mixed with a gold salt growth solution, rod-shaped micellar template (cetyltrimethylammonium bromide; CTAB), reducing agent (ascorbic acid), and small amounts of silver ions for shape induction to produce spheroid or rod-like GNPs. They also improved this methodology to produce monodisperse, multiple-shaped GNPs [25, 26]. Other methods for synthesizing GNPs include galvanic replacement reaction (gold nanocages) [27-30], and photochemical reduction (cubic GNPs) [31].

2.2. Targeting Moieties

Targeting moieties currently used are monoclonal antibodies (mAbs), antibody fragments, peptides, proteins, aptamers, and small molecules (Fig. **4**) [15].

0929-8673/11 $58.00+.00

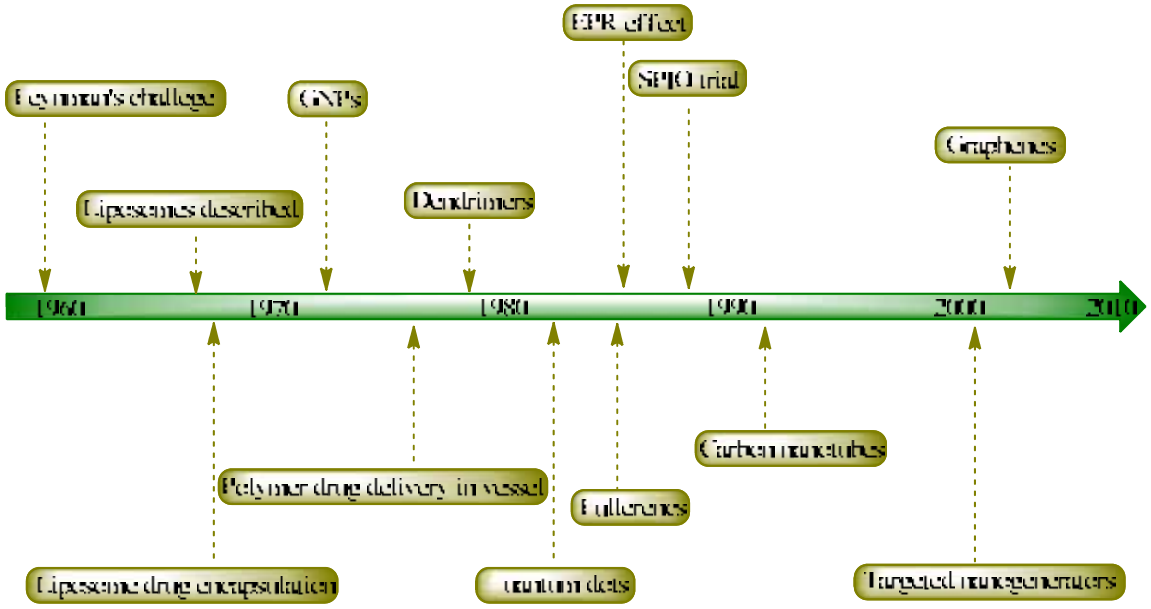

Fig. (1). Development of nanoplatforms for cancer imaging and therapy (abbreviations: EPR, enhanced permeability and retention; SPIO, superparamagnetic iron oxide) (adapted from Refs. [8, 11, 12]).

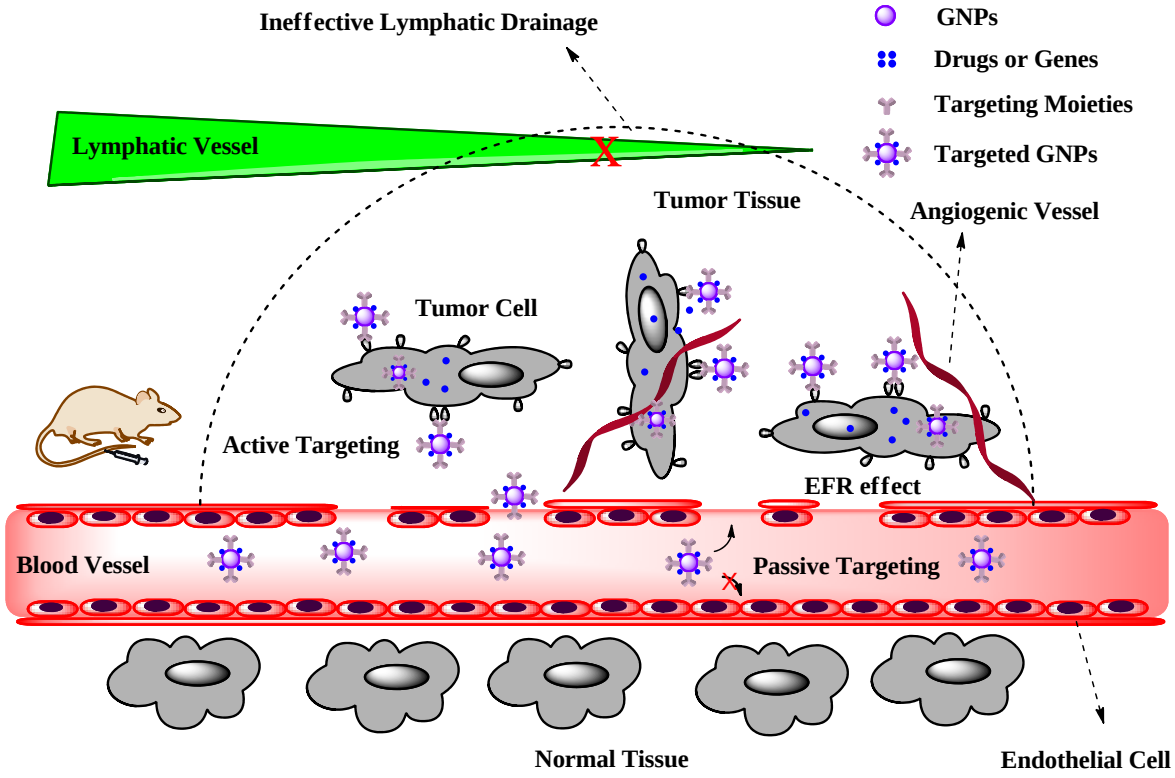

Fig. (2). A schematic diagram showing the mechanism of passive tissue targeting and active cellular targeting (adapted from Refs. [15, 20]).

In the last 25 years, 10 anticancer mAbs have been approved by the Food and Drug Administration (FDA) for clinical use [34]. Although some antibodies such as Mylotarg™ have been withdrawn from the market [35], mAbs are still the preferred class of targeting moieties. However, the Fc domain of an intact mAb can also bind to the Fc receptors on normal cells, as in the case of macrophages. This may lead to increased immunogenicity and evoke an immune response, leading to uptake of nanocarriers by the liver and spleen [15]. Because of these limitations and challenges in using whole antibodies, there is an increasing interest in using antibody fragments to improve tumor penetration but retain a high antigen-binding specificity [36]. These include the monovalent (Fab, scFv, single variable V_H and V_L domains), bivalent [F(ab')$_2$, diabodies, minibodies, etc.], and multivalent fragments.

Peptides are becoming attractive targeting molecules because of their high specificity, high affinity, small size, low immunogenicity,

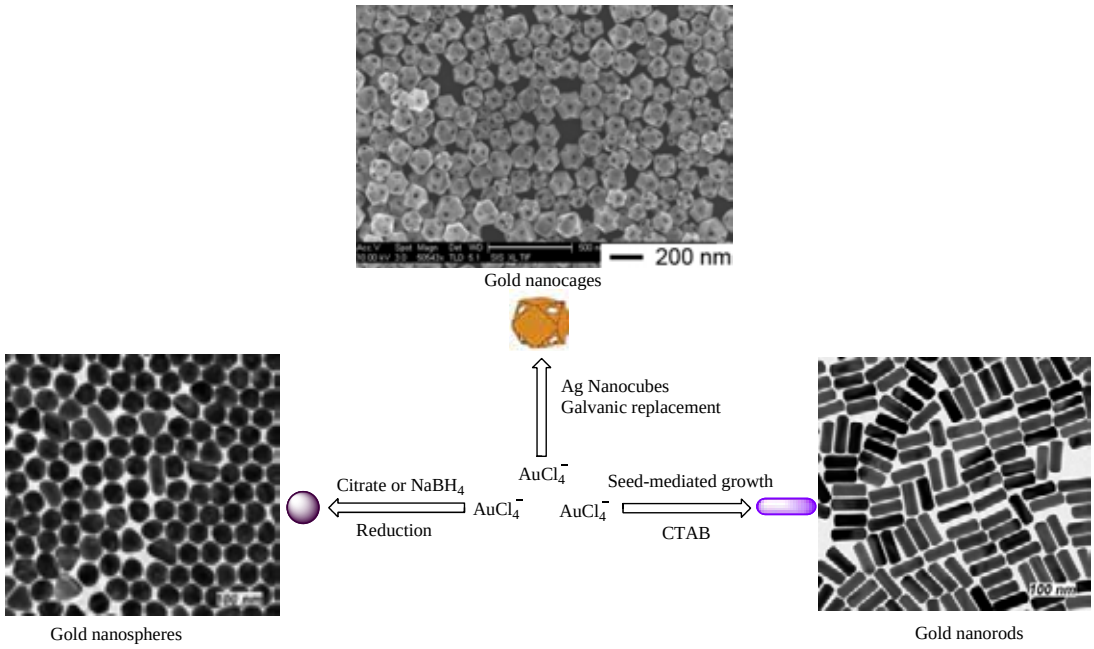

Fig. (3). Synthetic methods and transmission electron microscopy (TEM)/scanning electron microscopy (SEM) images of current GNPs: gold nanospheres (adapted from Ref. [32], with permission from the American Chemical Society; copyright 2008), gold nanorods (adapted from Ref. [33], with permission from the American Chemical Society; copyright 2008), and gold nanocages (adapted from Ref. [27], with permission from the American Chemical Society; copyright 2008).

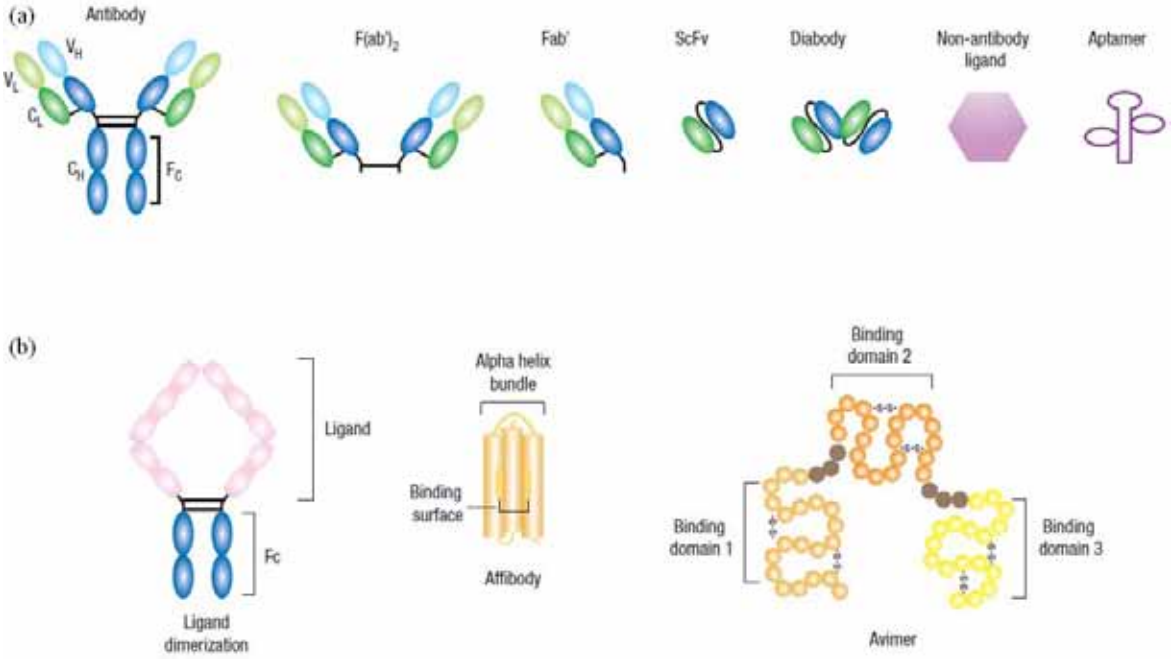

Fig. (4). Common targeting agents and ways to improve their affinity and selectivity. **(a)** The panel shows a variety of targeting molecules such as a monoclonal antibody or antibody fragments, nonantibody ligands, and aptamers. The antibody fragments F(ab')2 and Fab' are generated by enzymatic cleavage whereas the Fab', scFv, and bivalent scFv (diabody) fragments are created by molecular biology techniques. V_H: variable heavy chain; V_L: variable light chain; C_H: constant heavy chain; C_L: constant light chain. Nonantibody ligands include vitamins, carbohydrates, peptides, and other proteins. Aptamers can be composed of either DNA or RNA; **(b)** Affinity and selectivity can be increased through ligand dimerization or by screening for conformational-sensitive targeting agents such as affibodies, avimers and nanobodies, as well as intact antibodies and their fragments (adapted from Ref. [15], with permission from the Nature Publishing Group; copyright 2007).

high stability, and easy preparation. Some tumor-homing peptides, which are targeted specifically to tumor blood vessels, lymphatic vessels and/or tumor cells, have been isolated [37, 38]. The use of peptides as targeting moieties, such as Arg-Gly-Asp (RGD)

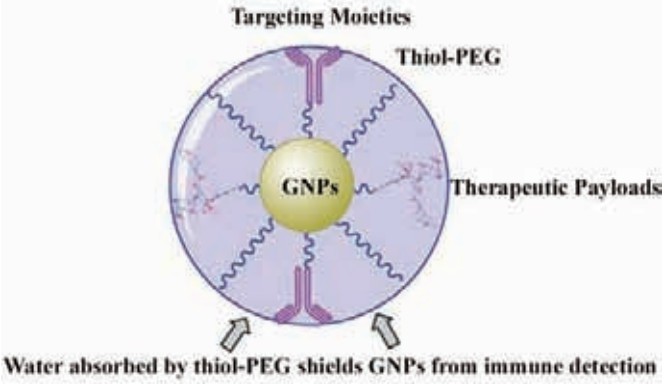

Fig. (5). Diagram of multifunctionalized gold nanoparticles.

sequence containing peptides, have been shown to cause increased intracellular drug delivery in different murine tumor models [39]. However, RGD also binds to other integrins such as $\alpha_5\beta_1$ and $\alpha_4\beta_1$ and is therefore not very specific to cancer cells, which may be harmful to normal tissues and thereby limit its use.

Proteins, including human serum albumin (HSA), transferrin and lectins, have been used as targeting moieties, drug-delivery systems, or both [40-42]. However, expression of their receptors or targets is not restricted to tumor tissues, which may pose harm to normal tissues.

Aptamers are single-stranded DNA or RNA oligonucleotides that fold into well-defined 3D structures and can be selected to bind to a wide variety of targets, such as intracellular proteins, transmembrane proteins, soluble proteins, carbohydrates, and small molecular drugs [43-45]. Aptamers routinely achieve the same affinities and specificities as therapeutic antibodies do, but without the immunogenicity concerns of protein drugs. Several aptamers have been developed to bind specifically to receptors on cancer cells [46], and thus may be suitable for preparing aptamer multifunctionalized GNPs. However, aptamers have not yet proven viable in the therapeutic arena as their high molecular mass and complex syntheses make them more expensive to manufacture than small molecules. Moreover, their still largely unknown pharmacokinetic properties make them harder to develop than any given therapeutic antibody [47].

Small molecules have shown great promise as a class of targeting molecules because of their small size and low cost of production. Folic acid (FA) and biotin are the 2 of the most extensively studied small molecules [48-52]. Because of the binding between targeting molecules on GNPs and receptors on the surface of cancer cells, GNPs can be selectively taken up by cancer cells.

However, most commonly targeted receptors such as folate receptors (FRs) are expressed not only on tumor cells but also on normal tissue cells, which will causes unintended uptake of small molecules in normal cells. Nonspecific binding and specific binding to nontargeting cells can diminish the effectiveness of targeting molecules. Alternatively, cancer cells typically overexpress multiple surface receptors. The dual-ligand targeting approach has been used to enhance cancer-targeting specificity. Efforts have been made to target FRs/EGFR (epidermal growth factor receptor) [53], transferring receptor/glucose transporter [54], and $\alpha_v\beta_3$ intergrin/galectin-1 receptor [55]. Our group has shown that dual-ligand GNPs with FA and glucose can enhance cell recognition, which enables them to kill human epidermal cancer cells (KB cells, FRs positive) under X-ray irradiation at a dose that is safe to FRs low-expression (such as normal) cells [56]. Without knowing the surface receptor profiles on cancer cells, we identified highly selective nanoparticles decorated with dual-targeting molecules by scanning the cell surface with a dual-ligand GNPs array, which varies the molecular diversity of the secondary ligands that surround the primary ligand on GNPs [57]. We demonstrated that this approach can be used to differentiate among cells that have different surface receptors profiles surrounding a common primary receptor expressed at high or low levels. The sensitive differentiation of cells with high expression of a common primary receptor with different secondary receptor profiles may be potentially used to individualize treatment for patients.

2.3. Therapeutic Payloads

GNPs have provided nontoxic carriers for drug and gene delivery applications [58]. Several types of therapeutic agents such as proteins, peptides, nucleic acids, and small- molecule drugs have been conjugated to GNPs to form GNPs-based nanodrugs (Fig. **5**) [59].

In an *in vivo* study, Paciotti *et al.* investigated the therapeutic effect of PEG-coated GNPs with adsorbed tumor necrosis factor (CYT-6091, GNPs-TNFs) [60, 61]. When GNPs-TNFs were injected intravenously into mice, they rapidly accumulated in MC-38 colon carcinoma tumors and show little to no accumulation in livers, spleens (i.e. the RES) or other healthy organs. TNFs provided both targeting and therapeutic action to kill the targeted cells. Importantly, the particles were more effective than "free" TNFs at reducing tumor mass.

GNPs-based nanodrugs such as CYT-6091 (GNPs-TNFs), CYT-21001 (GNPs-TNFs-paclitaxel), CYT-31000 (GNPs-TNFs-doxorubicin), CYT-41000 (GNPs-TNFs-IL12), and CYR-51000 (TNFs-IL2) have been tested in clinical trials [62-67]. Preliminary data from the phase I study [63] indicates that CYT-6091 is seen in tumors but not in surrounding healthy tissue, and that the mechanism of targeting solid tumors is independent of tumor type. To date CYT-6091 has not affected renal, liver or immune function and no unexpected serious adverse events have been reported. CYT-6091 induces a predictable and controllable febrile response, but not yet induced hypotension, the dose-limiting toxic effect of TNFs.

2.4. Advancements in Radiotherapy and Computed Tomography (CT) Imaging

Radiotherapy remains a major modality of cancer therapy, but can cause significant biological damages, as it can also induce degradation of healthy tissues. Hence, for the last 5 decades, efforts have been devoted to increase its efficiency and tolerance, such as better dose fractionation schedules or tomotherapy (radiation delivered slice by slice). Despite these advances, normal tissue toxicity remains a dose-limiting factor in clinical radiation therapy [68]. Computed tomography (CT) is currently one of the most useful diagnostic tools in hospitals in terms of availability, efficiency, and cost. Conventional iodine-based contrast agents

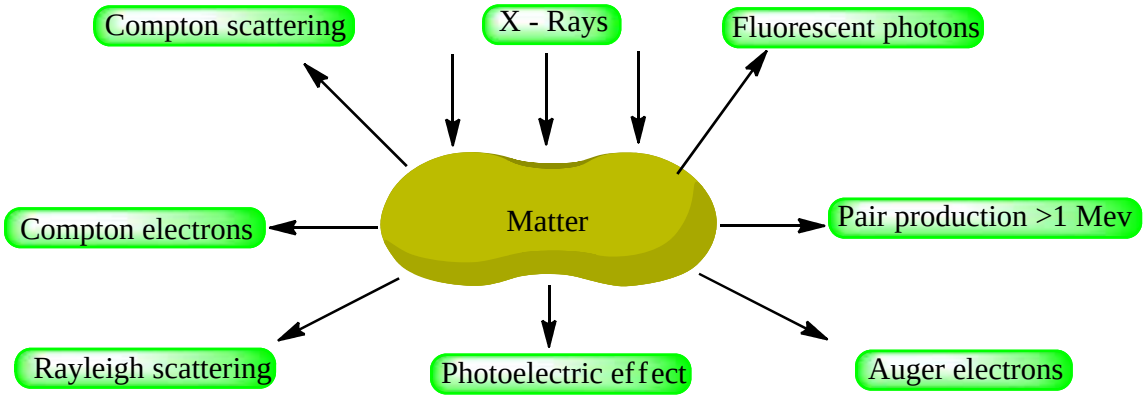

Fig. (6). Schematic diagram of interaction of X-rays with matter.

allow only very short imaging times because of rapid renal clearance, renal toxicity, and vascular permeation [69]. X-ray radiation therapy and CT imaging techniques are based on the use of X-rays. When X-rays impinge on matter, several interactions such as scattered photons (X-rays), photoelectrons, compton electrons, auger electrons and fluorescence photons can occur (Fig. **6**), leading to radiochemical (free radical and ionization) damage to the tissues [70]. Gold is an excellent absorber of X-rays (100 keV: gold, 5.16 cm^2 g^{-1}; iodine, 1.94 cm^2 g^{-1}) [71] and the X-ray attenuation of GNPs is found to be much higher than that of the iodine-based contrast agent at the same molar concentration [72]. Consequently, GNPs have been used as radiotherapy enhancement [73-77] and CT imaging contrast agents [69, 71, 78-82] *in vitro* and *in vivo*.

3. FABRICATION OF MULTIFUNCTIONALIZED GNPS

Targeting moieties and therapeutic payloads can be noncovalently or covalently conjugated to GNPs to form multifunctionalized GNPs. The noncovalent conjugation method has the main advantage of being simple and applicable to almost any type of targeting moiety or therapeutic drug. Covalent conjugation may reduce molecular rearrangements and conformation changes, provide cleavable bonds, and allow directional arrangement of molecules on the surface of GNPs.

3.1. Noncovalent Conjugation of Targeting Moieties and Drugs to GNPs

Noncovalent conjugations of targeting moieties or therapeutic drugs to GNPs form weak interactions between molecules and GNPs. These interactions include electrostatic interactions, hydrogen bonds, hydrophobic and van der Waals interactions (Scheme **1**) [83]. Noncovalent conjugation is simple and can be applied to almost any type of targeting moiety or therapeutic drug. Various noncovalent conjugates have been developed to detect tumor markers and enhance CT imaging effect [78, 84-90]. However, noncovalent conjugation may lead to molecular rearrangements and conformation changes, which may result in a loss of their biological properties. The physical adsorption of proteins is in general not sufficient to stabilize bare GNPs, and bare GNPs are, in general, unstable in physiological solutions [90].

3.2. Covalent Conjugation of Targeting Moieties and Drugs to GNPs

Covalent conjugation is commonly achieved through thiol chemistry, through the formation of strong Au-S bond. Antibody, antibody fragment, peptide, proteins, aptamers, and small molecules have been used to fabricate multifunctionalized GNPs. Antibodies, antibody fragments, peptides, and proteins have the similar modifiable groups (-NH_2, -SH, -COOH, -OH) on their surface,

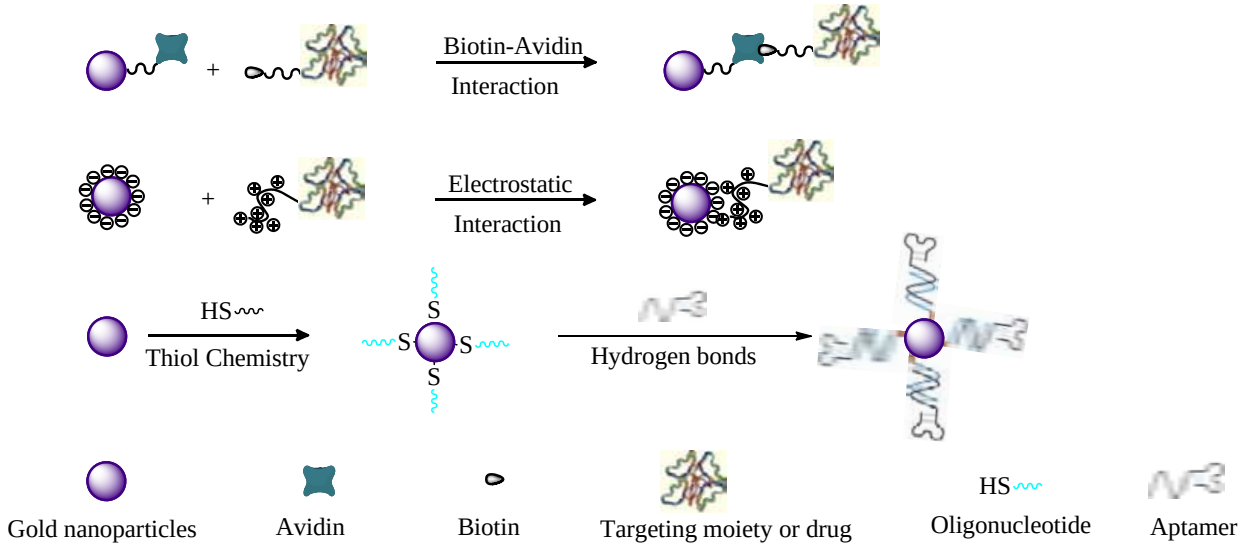

Scheme 1. Synthetic routes for the noncovalent conjugation of targeting moieties or drugs to GNPs.

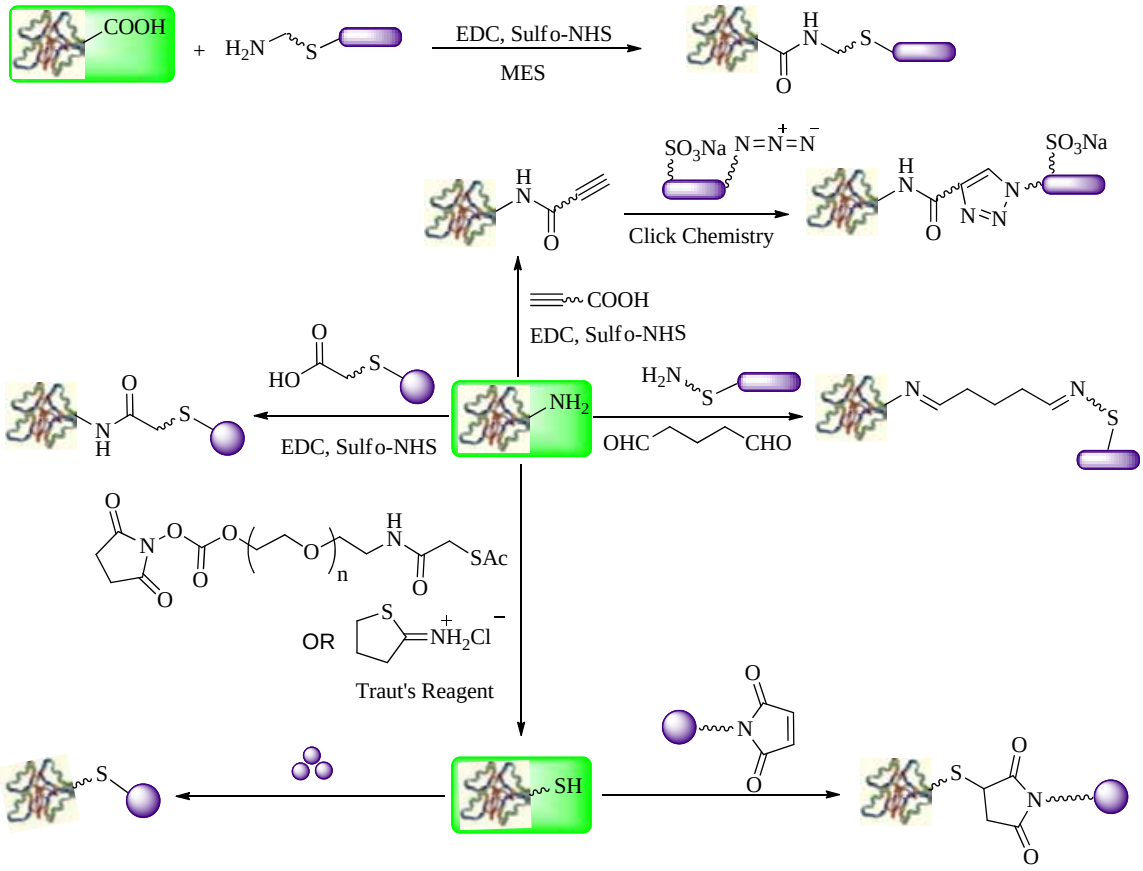

Scheme 2. Synthetic routes for the random conjugation of antibodies, antibody fragments, peptides, or proteins to GNPs.

which destines that these molecules possess the same covalent conjugation methods. Most aptamers are conjugated to GNPs after being modified by thiol group-containing linkers. Some small molecules such as therapeutic payloads can be conjugated to GNPs through cleavable bonds. Combinatorial surface modification has also been achieved by using these methods.

3.2.1. Conjugation of Antibody, Antibody Fragment, Peptide, and Protein to GNPs

Random Conjugation

The clear advantage of using covalent linkages over physical adsorption is that covalent linkages prevent the competitive displacement of the adsorbed targeting moieties by blood components [91]. Antibody, antibody fragment, peptide, and protein can be covalently conjugated to GNPs *via* the formation of strong Au-S bond [9, 92-94]. To improve circulation time and binding efficiency and reduce immunogenicity, use of spacers such as PEG units is also recommended. Spacers can be covalently linked at one end to GNPs *via* Au-S bond and at the other end with amine groups by using EDC/NHS chemistry [20, 29, 95-102], the well-established glutaraldehyde spacer method [103, 104], click chemistry [105, 106], or the maleimide method [107] (Scheme **2**).

Directional Conjugation

Amine groups on the surface of antibody, antibody fragment, peptide, and protein may be a part of active sites; consequently, their random modification may reduce the recognition ability. Directional conjugation may provide a strategy to maximize targeting moieties functionality. For example, antibodies, which are glycoproteins, have been conjugated to GNPs through the Fc region, where the polysaccharides are present. A heterobifunctional linker, hydrazide-polyethylene glycol-dithiol, is used to directionally attach the Fc or nonbinding region of the antibodies to the GNPs surface [108, 109] (Scheme **3**). It is also possible to achieve a directional conjugation using the following bonds: aldehydes to the lysine-rich region of targeting moieties; epoxides to the histidine-rich region of the targeting moieties and thiol to the centre thiol groups of the targeting moieties obtained by reduction [91].

3.2.2. Conjugation of Aptamers to GNPs

Covalent conjugation of aptamers to GNPs can also be achieved most commonly through Au-S bond [110-112]. The aptamer is typically modified to carry a terminal thiol group, which is in turn conjugated to the surface of the GNPs or maleimide functional groups present on the surface of GNPs. To enhance drug-loading capacity, one part of oligonucleotide is often fused to the targeted aptamers (Scheme **4**) [81].

3.2.3. Conjugation of Small Molecules to GNPs

Generally, small-molecule targeting moieties or drugs can be covalently conjugated to GNPs through Au-S bond by using various organic reactions. For example, covalent conjugation of FA or therapeutic drugs to GNPs can be achieved through succinimidyl ester amine chemistry, which results in a stable amide linkage (Scheme **5**) [50-52]. FA must be conjugated to nanoparticles *via* its γ-carboxyl group in order to retain its receptor-binding activity [113]. Therefore, conjugation of FA to the surface of nanoparticles primarily focuses on reactions of the carboxyl group [114, 115].

3.2.4. Combinatorial Surface Modification

Chemical modification on the surface gives GNPs unique physicochemical properties and, therefore, biological activities, such as targeting properties. However, the conventional one-at-a-time chemistry approach does not allow rapid identification of ideal

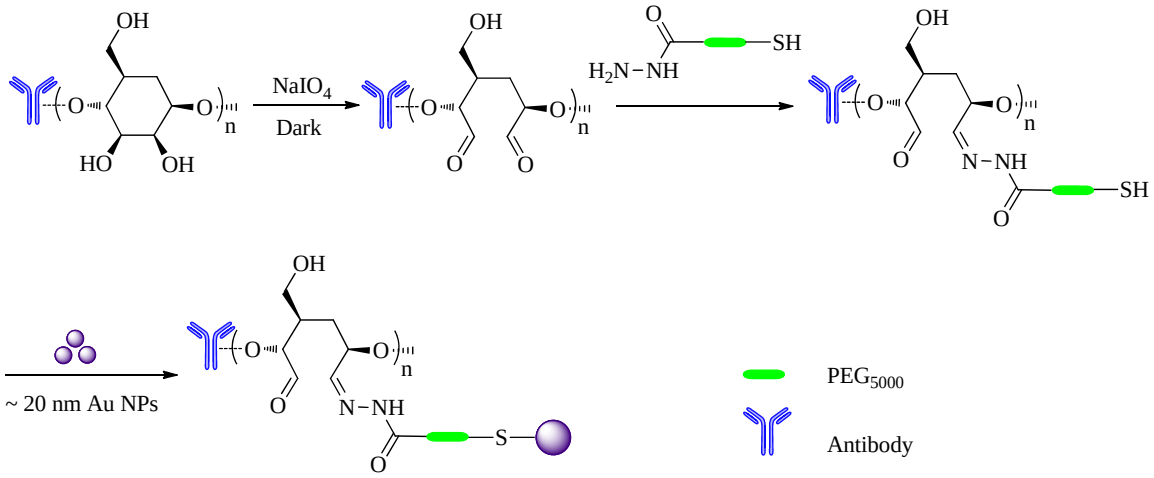

Scheme 3. Synthetic route for the directional conjugation of antibodies to GNPs.

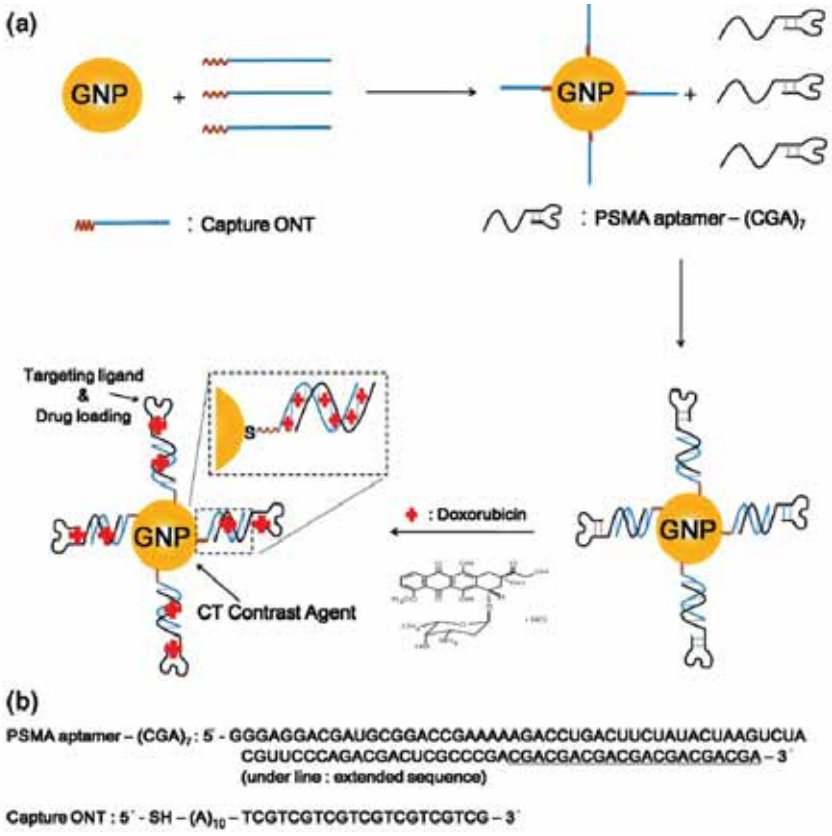

Scheme 4. (a) Synthetic route for preparing Dox-loaded aptamer-conjugated GNPs. **(b)** PSMA aptamer and ONT sequences used to synthesize Dox-loaded aptamer-conjugated GNPs (adapted from Ref. [81], with permission from the American Chemical Society; copyright 2010).

GNPs. To accomplish this without a priori knowledge of multiple targets, nano combinatorial chemistry, a system of rational design, combinatorial synthesis and high-throughput screening offers ideal opportunities in the burgeoning field of nanomedicine. Nanocombinatorial chemistry enables (1) searching for an initial lead through rational design, combinatorial synthesis, and high-throughput screening, and (2) once a lead is available, optimizing the lead in order to meet a set of criteria for nanomedicine candidate. We have reported the development of a dual-ligand GNPs (DLGNP) array to differentiate between cells that have different surface receptor profiles surrounding a common primary receptor [57]. We synthesized DLGNP by using FA as primary targeting ligand and making the secondary ligand from a combinatorial array (Scheme **6**). Cell recognition was investigated in 4 cell lines with various expression levels of FRs and totally unknown receptor profiles considering secondary receptors. We found a marked difference in cell binding and uptake of DLGNP in different cells suggesting the different receptor profiles surrounding FRs. Furthermore, multivalent bindings of DLGNP allow differentiation of cells with high and low expression of FRs and enhance the contrast between these cells in radiation-induced cell death measurements. These powerful enhancements of cell recognition and discrimination make nanoparticles powerful candidate for developing personalized and safe medication for drug delivery and radiation therapy.

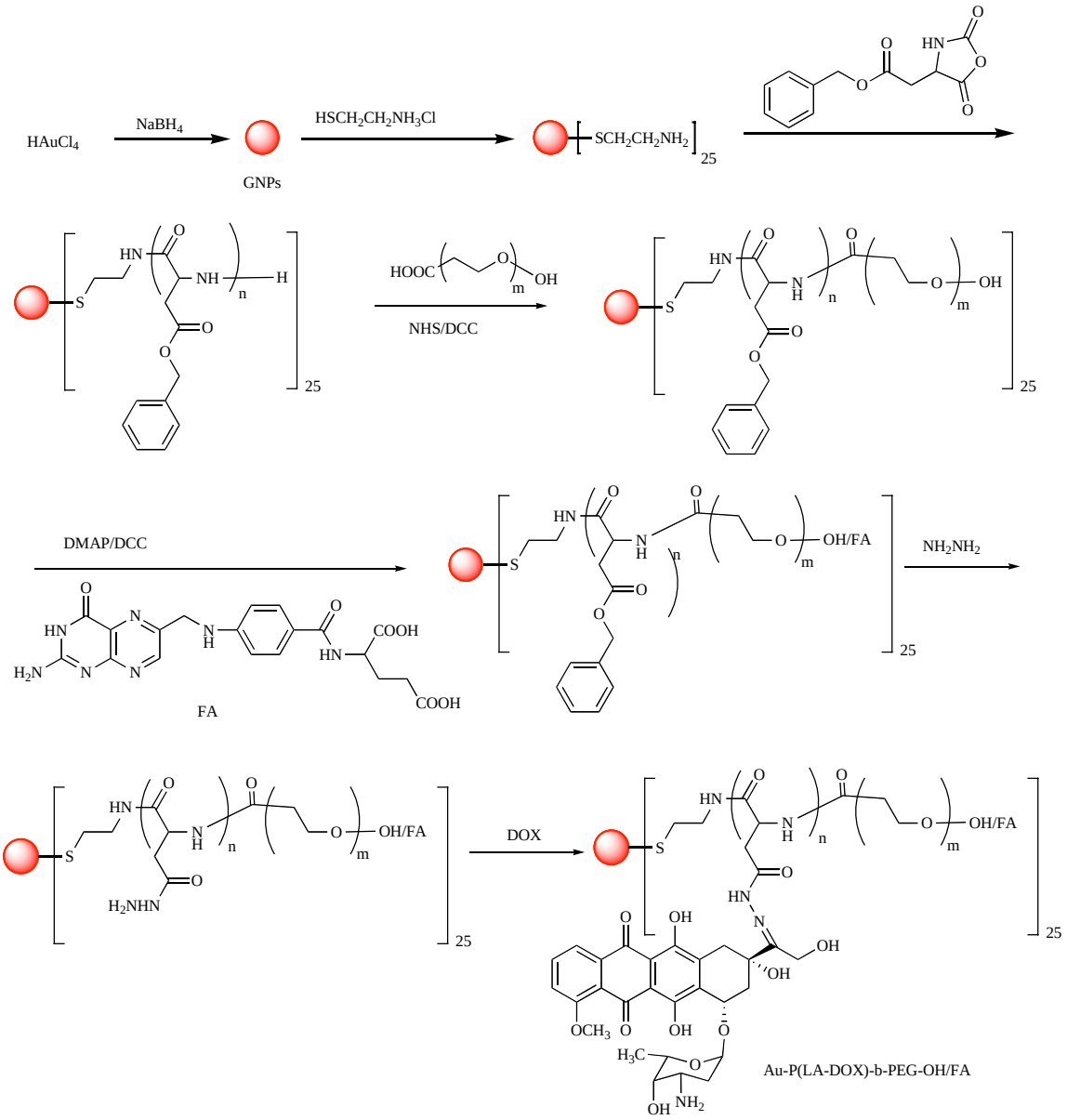

Scheme 5. Synthetic route for the conjugation of FA and DOX to GNPs (adapted from Ref. [50], with permission from the Elsevier Ltd; copyright 2009).

4. APPLICATION OF MULTIFUNCTIONALIZED GNPS IN IMAGING

GNPs possess many unique features and have been investigated for various applications in imaging, such as in CT, surface-enhanced Raman spectroscopy (SERS), and photoacoustic imaging (PAI). After functionalized with targeting moieties, GNPs gain the molecular imaging potential for cancer diagnosis.

4.1. Enhanced CT Imaging Agents

Several studies have used GNPs as CT contrast agents *in vivo* [71, 78, 79]. Compared with eXIA 160 (an iodine-based contrast agent), heparin-coated GNPs give better liver-specific CT images *in vivo* (Fig. **7**). The outstanding properties of this platform system highlight its potential as a novel liver-specific CT imaging agent and a molecular imaging probe for assessment of the therapeutic effect of anticancer drugs against liver cancer by a noninvasive method [78].

Currently, CT is not a molecular imaging modality because relevant targeted and molecularly specific contrast agents have not yet been developed. To date, 3 types of targeted GNPs (antibody-GNPs, aptamer-GNPs, and deoxyglucose-GNPs) have been reported as molecular CT imaging contrast agents *in vitro* [69, 81, 82]. We expect that the CT molecular imaging technique will revolutionize modern cancer diagnosis and staging by allowing the reliable and sensitive detection of lymph nodes and other metastases, which are not available today.

4.2. Surface-enhanced Raman Spectroscopy (SERS) and Imaging

Raman imaging holds significant potential as a strategy for biomedical imaging of living individuals. The Raman spectra and Raman images of methylene blue molecules adsorbed as a single layer on gold nanospheres were found useful to study plasmon properties [116]. After this, 2 groups have independently reported the *in vivo* targeted imaging of cancer by using Raman spectroscopy and SERS nanoparticles. One study showed that small-molecule Raman reporters (such as fluorescent dyes) were stabilized by thiolated PEG and gave large optical enhancements

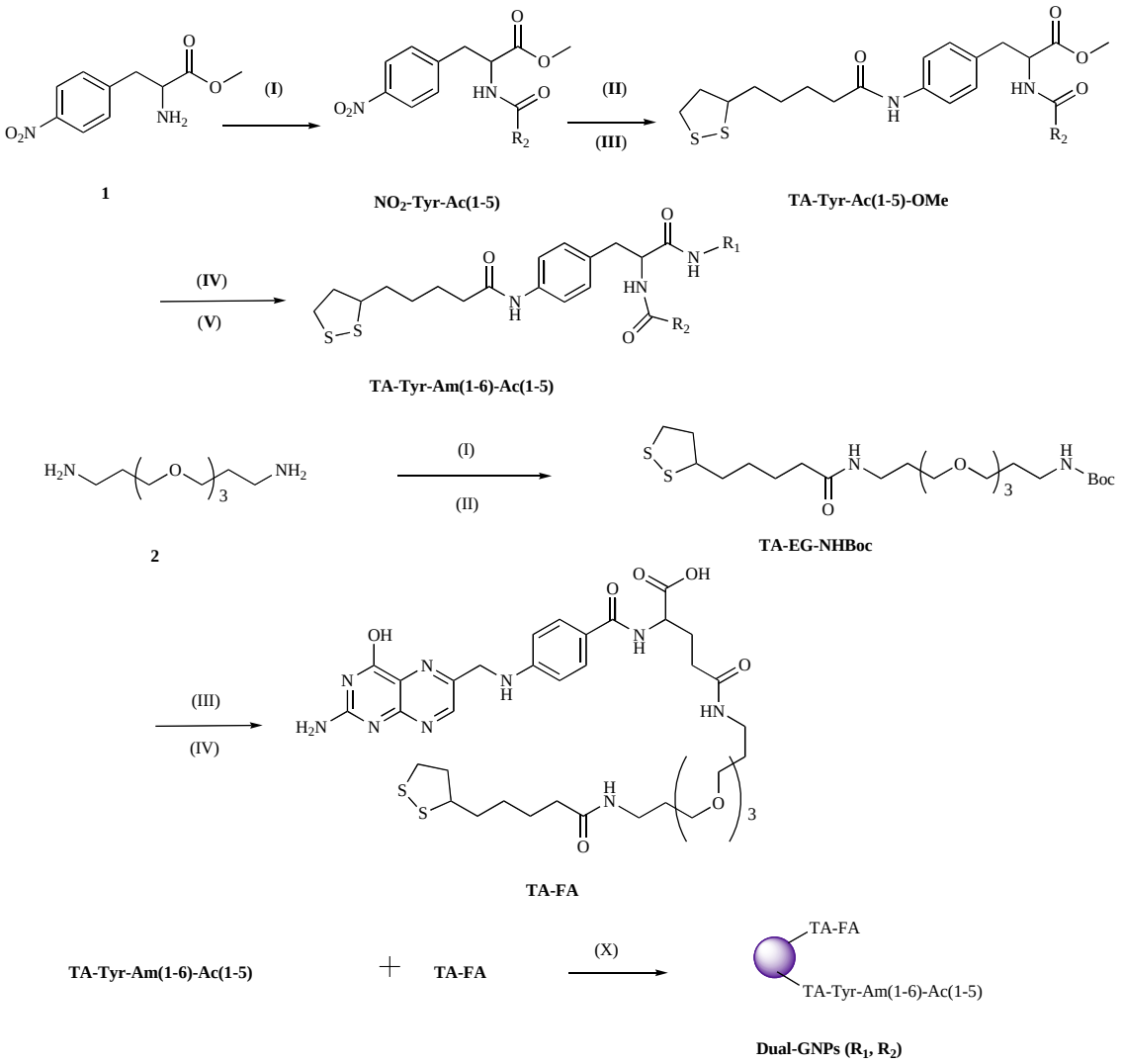

Reagents and conditions: (I) R_2-COCl, TEA, DCM; (II) Zn, AcOH, EtOH; (III) Oxalyl chloride, DMF, DCM, Thioctic acid, TEA; (IV) LiOH, H_2O, THF; (V) R_1-NH_2, DCC, NHS, THF; (VI) Boc_2O, NEt_3, MeOH; (VII) Thioctic acid, DCC, NHS, THF; (VIII) TFA/DCM, 1:4; (IX) Folic acid, DCC, Py, DMSO; (X) $HAuCl_4 \cdot 3H_2O$, $NaBH_4$,MeOH/H_2O.

Scheme 6. Synthetic route for dual-ligand GNPs library. Thioctic acid is used as the linker molecule between GNPs surface and both the primary targeting reagent (FA) and the secondary ligand. Six amines and five acyl chloride were selected to construct a library with 30 members (adapted from Ref. [57], with permission from the American Chemical Society; copyright 2010).

[20]. When conjugated to tumor-targeting ligands, the conjugated SERS nanoparticles were able to target tumor markers such as EGFR on human cancer cells and in xenograft tumor models (Fig. **8**). In another study, SERS nanoparticles composed of a gold core, a Raman-active molecular layer, and a silica coating were used for Raman imaging *in vivo* [117]. A minimum detection sensitivity of 8 pM of SERS nanoparticles was observed in a living mouse. As a proof-of-principle, *in vivo* multiplexed imaging of 4 different SERS nanoparticles was also demonstrated.

4.3. Photoacoustic Imaging (PAI)

Photoacoustic imaging (also called optoacoustic or thermoacoustic imaging), as a hybrid biomedical imaging modality, is developed based on the photoacoustic effect. In photoacoustic imaging, non-ionizing laser pulses are delivered into biological tissues (when radio frequency pulses are used, the technology is referred to as thermoacoustic imaging). Some of the delivered energy will be absorbed and converted into heat, leading to transient thermoelastic expansion and thus wideband (e.g. MHz) ultrasonic emission. The generated ultrasonic waves are then detected by ultrasonic transducers to form images [118]. Several types of GNPs have been used as contrast agents in photoacoustic imaging because of their unique optical absorption properties [67, 119-125]. [Nle^4, D-Phe^7]-α-MSH, a melanoma-specific peptide, functionalized gold nanocages (AuNCs) are compared with PEGylated gold nanocages for their accumulation in tumors, using the noninvasive PAI technique (Fig. **9**) [124]. Fig. (**9a**) shows the PAI signal enhancement in the melanomas as a function of postinjection time. After 6 hours, the targeting efficiency of [Nle^4, D-Phe^7]-α-MSH-AuNCs was approximately thrice that of PEG-AuNCs. The results agreed with those from ICP-MS analyses of the gold content present in the tumors (Fig. **9b**).

Photoacoustic imaging can provide 2D or 3D images of the targeted areas and has the potential to image human organs, such as the breast and the brain, with simultaneous high contrast and high spatial resolution [126]. Current studies on PAI contrast nanoparticles are focused on adding more features and optimizing

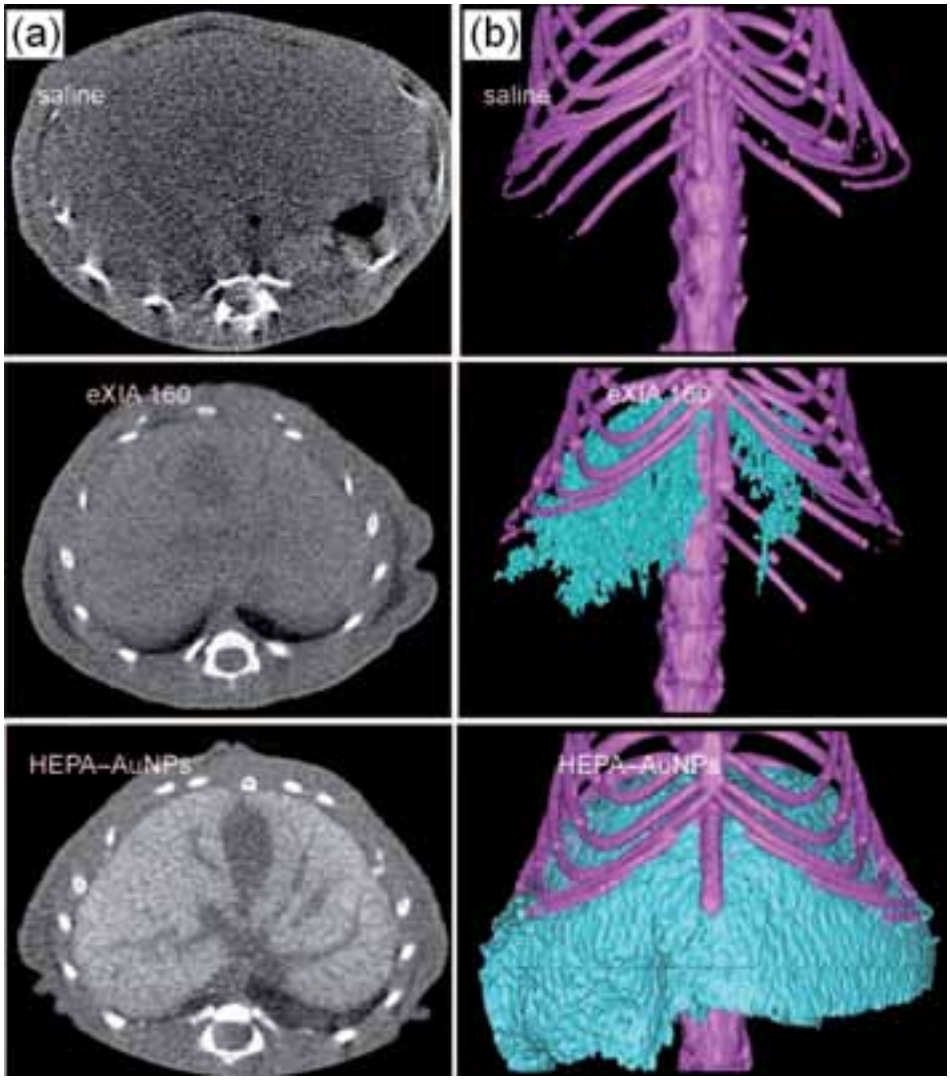

Fig. (7). (a) Cross-sectional micro-CT images in livers 2 h postinjection of saline, eXIA 160 (800 mg I kg^{-1}), and HEPA-GNPs (250 mg Au kg^{-1}); **(b)** Three-dimensional micro-CT images of livers obtained after 2 h post injection of saline, eXIA 160, and HEPA-GNPs (adapted from Ref. [78], with permission from the Wiley-VCH Verlag GmbH & Co. KGaA; copyright 2009).

absorption properties. The next generation of PAI contrast agents is expected to combine seamless detection and therapy capabilities [120].

5. APPLICATIONS OF MULTIFUNCTIONALIZED GNPs IN THERAPY

Multifunctionalized GNPs have been developed to deliver drugs in a controlled manner. Hyperthermia-induced cytotoxicity and enhanced radiation-induced cell death of GNPs enable multifunctionalized GNPs to be used as photothermal-therapy and radio-therapy sensitizers.

5.1. Drug Delivery

Multifunctionalized GNPs can target therapeutic payloads to tumor tissues through active targeting. After being internalized by tumor cells, therapeutic payloads can be released into the tumor cells in a controlled manner.

5.1.1. Targeted Drug Delivery and Body Distribution

Several studies on the therapeutic applications of active targeted GNPs reveal that drugs can be delivered to tumors through active targeted GNPs [9, 20, 60, 61, 100, 127-129]. In a study of the biodistribution of CYT-6091 (GNPs-TNFs) in a prostate tumor bearing mice model, Bischof *et al.* [127] found that the 2 components of CYT-6091 (TNF-α and GNPs) exhibited different *in vivo* behavior, with active TNF-α sequestering preferentially inside the tumor within the first 4 h after injection. GNPs accumulated in liver and spleen primarily between 4 and 24 h postinjection. The amount of GNPs in the liver gradually decreased over the duration of the study; only 35% of the injected gold was present in the organs tested at 4 months postinjection. Both the liver and spleen exhibited similar capacity per gram of tissue for GNPs uptake, although the liver took up most of the GNPs owing to its larger size.

5.1.2. Controlled Drug Release

Passive and active targeting can cause accumulation of multifunctionalized GNPs in tumor tissues. Several anticancer drugs, such as paclitaxel [130, 131], doxorubicin [50, 132] and platinum-based drugs [133, 134] have been covalently or noncovalently conjugated to GNPs to form multifunctionalized GNPs for cancer therapy. After internalized by tumor cells, multifunctionalized GNPs can release the entrapped therapeutic drugs in a controlled manner.

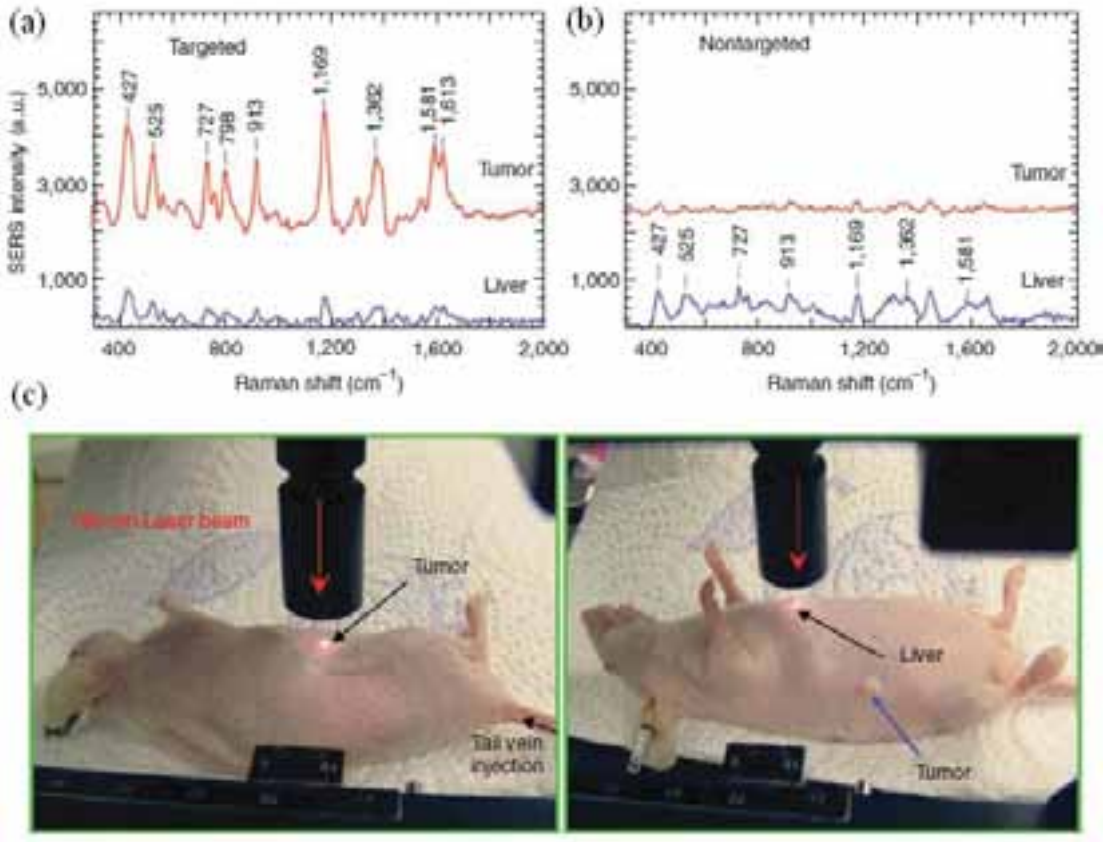

Fig. (8). *In vivo* cancer targeting and surface enhanced Raman detection by using ScFv antibody conjugated GNPs that recognize the tumor biomarker EGFR **(a, b)**. SERS spectra obtained from the tumor and the liver locations by using targeted **(a)** and nontargeted **(b)** nanoparticles. Two nude mice bearing human head-and-neck squamous cell carcinoma (Tu686) xenograft tumor (3-mm diameter) received 90 ml of ScFv EGFR-conjugated SERS tags or pegylated SERS tags (460 pM). The particles were administered *via* tail vein single injection. SERS spectra were taken 5 h after injection. **(c)** Photographs showing a laser beam focusing on the tumor site or on the anatomical location of liver. *In vivo* SERS spectra were obtained from the tumor site (red) and the liver site (blue) with 2-s signal integration and at 785 nm excitation. The spectra were background subtracted and shifted for better visualization. The Raman reporter molecule is malachite green, with distinct spectral signatures as labeled in **(a)** and **(b)**. Laser power: 20 mW (adapted from Ref. [20], with permission from the Nature Publishing Group; copyright 2008).

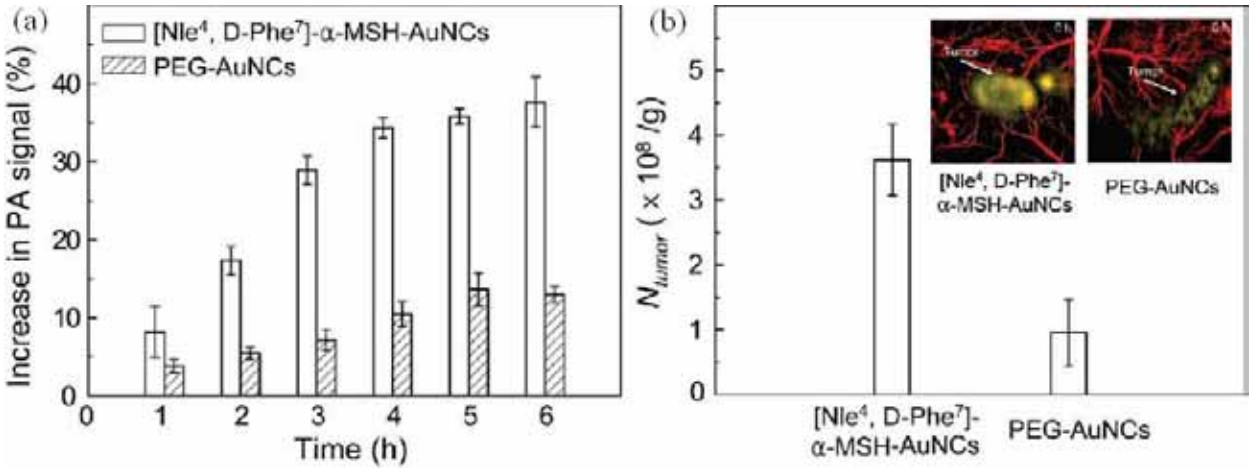

Fig. (9). (a) Time-course changes (%) in Photoacoustic imaging (PAI) amplitude after intravenous injection of [Nle^4, D-Phe^7]-α-MSH and PEG-AuNCs (n = 4 mice for each group). PAI signals increased up to 38 ± 6% for [Nle^4, D-Phe^7]-α-MSH-AuNCs while the maximum signal increase only reached 13 ± 2% for PEG-AuNCs at a post-injection time of 6 h ($p < 0.0001$). **(b)** The average number of AuNCs accumulated in the melanomas dissected at 6 h postinjection for the 2 types of AuNCs as measured by ICP-MS. N tumor denotes the number of AuNCs per unit tumor mass (g). The average number of [Nle^4, D-Phe^7]-α-MSH-AuNCs per tumor mass ($3.6 \pm 1.0 \times 10^8$ AuNCs g^{-1}) was 3.6 times (p = 0.02) that of PEG-AuNCs ($1.0 \pm 1.0 \times 10^8$ AuNCs g^{-1}). The inset shows the PAI of the melanoma at 6 h postinjection of [Nle^4, D-Phe^7]-α-MSH and PEG-AuNCs, respectively (Adapted from Ref. [124], with permission from the American Chemical Society; copyright 2010).

Glutathione-Mediated Release of Drugs

Intracellular glutathione (GSH) concentrations are substantially higher than extracellular concentrations, making selective intracellular release possible [135]. GSH can trigger the release of payload from the nanoparticle surface inside the cancer cells. In a recent study, Rotello *et al.* linked a hydrophobic dye (HSBDP) to GNPs as a model of drug. GSH-mediated release was detected in HepG2 cells by enhancement of the fluorescence signal (Fig. **10a**). In control experiments, low HSBDP release was found in mouse embryonic fibroblast cells which had 50% lower intracellular GSH levels than HepG2 cells [136, 137].

Photo-Regulated Release of Drugs

Drugs can be attached to GNPs through photo-switchable bonds. "Caged drugs" lose their activities by covalent linkages and their activities are restored upon photoirradiation [138, 139]. Nakanishi *et al.* demonstrated that GNPs with a photocleavable succinimidyl ester allow the delivery of amines to cells [140]. Lin *et al.* synthesized a gold-capped mesoporous silica nanoparticle (MSN) (Fig. **10b**); on photoirradiation, the photocleavable linker covalently attached to GNPs was cleaved resulting in the release of payloads [141].

pH-Mediated Release of Drugs

Cells can internalize particles from their surroundings and sort these particles to particular destinations. Most targeted GNPs are internalized by cancer cells *via* receptor-mediated endocytosis (RME) which generally occurs *via* clathrin/AP2 coated pits and vesicles. The locations of internalized GNPs are endosome-like and/or lysosome-like compartments, which are acidic organelles containing a battery of degradative enzymes [20, 142]. Accordingly, acid-sensitive linkers can be adapted for drug delivery and controlled release of drugs in cancer cells [143]. Gong *et al.* recently reported the synthesis of FA-conjugated amphiphilic GNPs with copolymers [50, 132]. The anticancer drug doxorubicin was conjugated onto the hydrophobic inner shell of GNPs *via* an acid-labile hydrazone linkage. The doxorubicin released rapidly at acidic surroundings (pH = 5.3 and 6.6) (Fig. **10c**), indicating that the GNPs-DOX conjugate can be a promising anticancer drug.

Enzyme-Mediated Release of Drugs

To overcome the lack of tumor specificity and low solubility in water, Hwu *et al.* incorporated paclitaxel by its thiol terminal onto colloidal GNPs through ligands exchange experiments (Fig. **10d**) [131]. A flexible PEG spacer was used to increase biocompatibility. Incorporation of the phosphodiester moiety in paclitaxel-containing nanoparticles enhanced the cancer-targeting capability. Dephosphorylation reactions in cancer cells liberated paclitaxel molecules from nanoparticles.

5.2. Hyperthermia-Induced Cytotoxicity

It has been recently shown that photothermal therapy by using the absorption properties of gold nanospheres [144-148], gold nanorods [149-153], and gold nanocages [128, 154-158], can selectively kill cancer cells. Nanorods are synthesized and conjugated to anti-EGFR monoclonal antibodies and incubated in

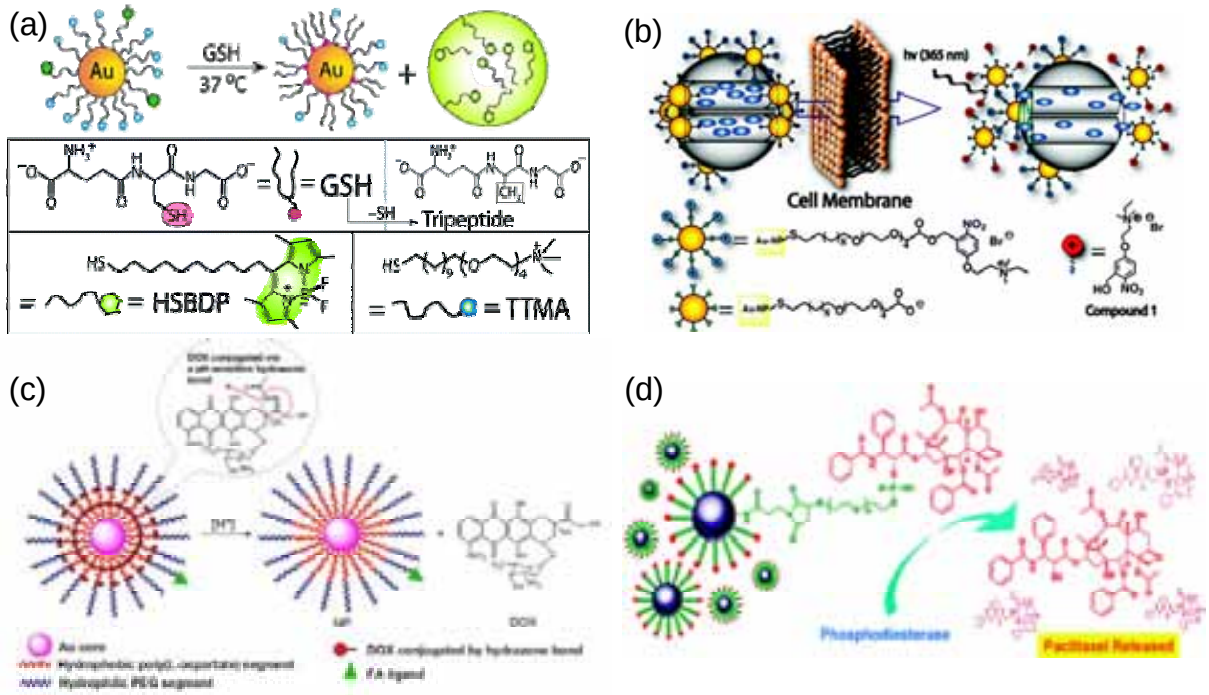

Fig. (10). (a) Structure of GNPs carrier and schematic depiction of the GSH-mediated surface monolayer exchange reaction which releases the payload, HSBDP (adapted from Ref. [136], with permission from the American Chemical Society; copyright 2006); **(b)** Upan UV irradiation, the photoabile linker on gold-capped mesoporous silica nanoparticles is cleaved, changing the surface charge property of GNPs from positive to negative. The charge repulsion between the GNPs and mesoporous silica nanoparticles then uncaps the mesopores and allows the release of guest molecules (adapted from Ref. [141], with permission from the American Chemical Society; copyright 2009); **(c)** The hydrazone linkage between the DOX and polymer on GNPs surface is prone to hydrolysis in an acidic condition. The release rate of DOX from the NPs will increase in the acidic environment of the endosomal intracellular compartments after they are internalized by cancer cells *via* the FA-mediated endocytosis (adapted from Ref. [50], with permission from the Elsevier Ltd; copyright 2009); **(d)** Dephosphorylation often occurs more easily in cancer cells than in normal cells. Hydrolysis of the phosphodiester moieties with the aid of phosphodiesterase can liberate free paclitaxel from GNPs (adapted from Ref. [131], with permission from the American Chemical Society; copyright 2009).

cell cultures with a nonmalignant epithelial cell line (HaCat) and 2 malignant oral epithelial cell lines (HOC 313 clone 8 and HSC 3). The targeted nanorods bind specifically to the surface of the malignant cells. After exposure to continuous red laser at 800 nm, malignant cells can be photothermally destroyed by approximately half the laser energy required for nonmalignant cells (Fig. **11**). Thus, both efficient cancer cell diagnostics and selective photothermal therapy are achieved simultaneously [149]. Small-size GNPs can be efficiently internalized by cancer cells through endocytosis. Kim *et al.* reported a smart GNPs that forms aggregates inside the cells if pH value is change [159]. The pH-induced formation of aggregates blocked the exocytosis by increased size and shifted the absorption to far-red and near-infrared, which thereby allowing maximal tissue penetration for potential therapeutic applications.

GNPs can also be used to deliver of photodynamic therapy (PDT) drugs. Most photosensitizing agents (e.g., phthalocyanines) are hydrophobic and limited by the side effects and long administration time (24 h to reach maximum accumulation in tumors). PEGylated GNPs-phthalocyanine conjugates act as a water-soluble and biocompatible cage that allows delivery of hydrophobic drugs to their sites of PDT action. With this conjugate, the drug administration time has been reduced to less than 2 h [160].

5.3. Enhancement of Radiation-induced Cell Death

More than 50% of the people who develop cancer each year receive radiation therapy as a component of their treatment. The concept of using high-Z materials to decrease the radiation dose during radiotherapy was introduced in the last decade after iodine was found to sensitize cultured cells [161]. Unfortunately, iodine radiosensitizers are not selective for cancer cells. Compared with iodine, gold has a higher Z number and better biocompatibility. Hainfeld *et al.* demonstrated that intravenously administered GNPs (1.9 nm) could deliver high concentrations of gold to tumors (up to 0.7 % weight %) with specificity and thereby improve X-ray therapy [162]. Later, several studies explored the enhanced cytotoxicity of X-ray radiation when different modified GNPs were used [163-167]. Chitarani *et al.* reported that GNPs, with a diameter of 50 nm, showed the highest radio-sensitization enhancement factor (1.43 at 220 kVp) compared to GNPs of 14 and 74 nm (1.20 and 1.26, respectively) [168].

6. IMPLICATIONS AND FUTURE DIRECTIONS

Passive and active targeting *via* nanoplatforms provides a promising approach for cancer imaging and therapy. The development of smart multifunctionalized GNPs that can deliver therapeutic drugs or contrast agents to tumors in a controlled manner may help improve the therapeutic index and imaging effect. However, current studies indicate that achieving a preferred accumulation of nanoparticles in the tumor tissue is still challenging because of the binding and clearance of GNPs in the liver, kidney, and spleen [9, 20, 60, 61, 100, 127-129]. Such a clearance decreases the targeting efficiency and is toxic to the organs. To achieve a more effective and specific accumulation of GNPs in tumor tissues, the size, shape, and surface properties of the targeted GNPs should be optimized. Likewise, novel structures used to evade the spleen, liver, and kidney clearance and the corresponding fabrication method should be developed in the near future.

Most cancer-targeting multifunctionalized GNPs can be internalized into tumor cells through endocytosis pathway (RME) and the intracellular localization of the GNPs is mostly endosome and lysosome-like compartments [20, 142]. Lysosomes are acidic organelles that contain a battery of degradative enzymes which can degrade nucleic acids and proteins into their monomeric subunits. In this microenvironment, small-molecule drugs can be released in a controlled manner. However, most of the macromolecules such as proteins and nucleic acids delivered through GNPs are degraded in these organelles, which decrease the delivery efficiency of proteins and nucleic acids. Therefore, novel multifunctionalized GNPs and the corresponding fabrication method should be developed to conquer these barriers for more efficient delivery.

GNPs have been extensively studied in CT, SERS, PAI, and other cancer imaging modalities, which can be used in conjunction with structural imaging techniques to diagnose, characterize, or monitor tumors before and after therapeutic intervention. CT is currently one of the most useful diagnostic tools in hospitals today in terms of availability, efficiency, and cost. Currently, CT is still

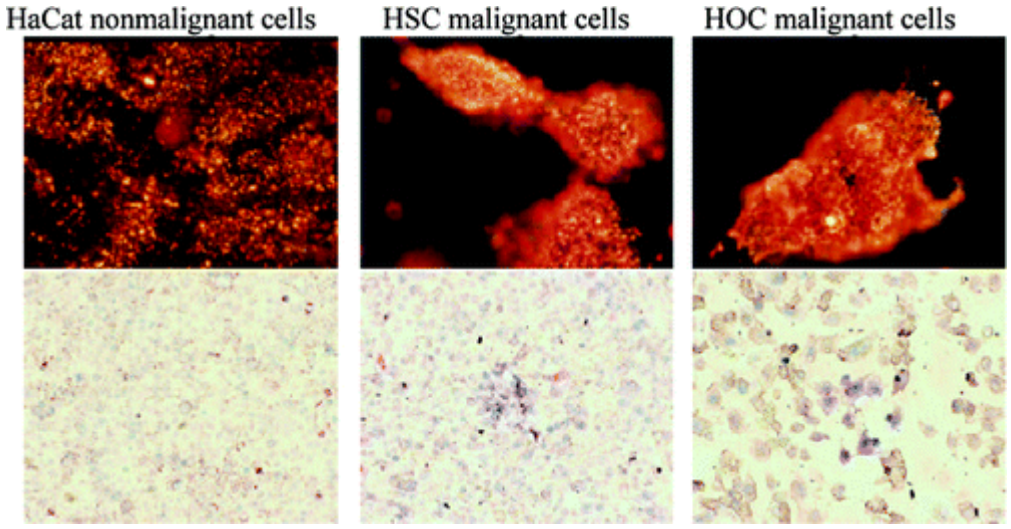

Fig. (11). Light-scattering images and photothermal therapy of cancer cells with anti-EGFR antibody conjugate Au nanorods. Light-scattering images are taken after incubation with Au nanorods for 30 min at room temperature. The anti-EGFR antibody-conjugated nanorods bind specifically to the surface of the malignant-type cells (HSC and HOC) compared with nonmalignant cells (HaCat) with a much higher affinity due to the overexpressed EGFR on the cytoplasmic membrane of the malignant cells. After exposure to laser irradiation at power values of 120 mW, HSC and HOC malignant cells are obviously injured but HaCat normal cells are not affected (adapted from Ref. [149], with permission from the American Chemical Society; copyright 2006).

not a molecular imaging modality as the relevant targeted and molecularly specific contrast agents have not yet been developed [69, 169, 170]. Moreover, current CT is not efficient in detecting tumors and metastases that are smaller than 5 mm [69, 171]. Future development of multifunctionalized GNPs will enable CT to image tiny tumor mass providing earlier diagnosis and quicker information on treatment effectiveness.

ACKNOWLEDGEMENTS

This work was supported by the National Basic Research Program of China (2010CB933504), National Natural Science Foundation of China (21077068 and 20975089), Innovation Projects of the Chinese Academy of Sciences (KZCX2-EW-206), the American Lebanese Syrian Associated Charities (ALSAC) and St. Jude Children's Research Hospital. We thank Vani Shanker for editing and checking the texts of all the manuscripts.

REFERENCES

[1] Heath, J.R.; Davis, M.E. Nanotechnology and cancer. *Annu. Rev. Med.*, **2008**, *59*(1), 251-265.

[2] Service, R.F. Nanoparticle trojan horses gallop from the lab into the clinic. *Science*, **2010**, *330*(6002), 314-315.

[3] Duncan, R. Polymer conjugates as anticancer nanomedicines. *Nat. Rev. Cancer*, **2006**, *6*(9), 688-701.

[4] Dinndorf, P.A.; Gootenberg, J.; Cohen, M.H.; Keegan, P.; Pazdur, R. FDA drug approval summary: pegaspargase (oncaspar(R)) for the first-line treatment of children with acute lymphoblastic leukemia (ALL). *Oncologist*, **2007**, *12*(8), 991-998.

[5] Dobrovolskaia, M.A.; McNeil, S.E. Immunological properties of engineered nanomaterials. *Nat. Nanotechnol.*, **2007**, *2*(8), 469-478.

[6] Davis, M.E.; Chen, Z.; Shin, D.M. Nanoparticle therapeutics: an emerging treatment modality for cancer. *Nat. Rev. Drug Discov.*, **2008**, *7*(9), 771-782.

[7] Lammers, T.; Hennink, W.E.; Storm, G. Tumour-targeted nanomedicines: principles and practice. *Br. J. Cancer*, **2008**, *99*(3), 392-397.

[8] Scheinberg, D.A.; Villa, C.H.; Escorcia, F.E.; McDevitt, M.R. Conscripts of the infinite armada: systemic cancer therapy using nanomaterials. *Nat. Rev. Clin. Oncol.*, **2010**, *7*(5), 266-276.

[9] Chanda, N.; Kattumuri, V.; Shukla, R.; Zambre, A.; Katti, K.; Upendran, A.; Kulkarni, R.R.; Kan, P.; Fent, G.M.; Casteel, S.W.; Smith, C.J.; Boote, E.; Robertson, J.D.; Cutler, C.; Lever, J.R.; Katti, K.V.; Kannan, R. Bombesin functionalized gold nanoparticles show *in vitro* and *in vivo* cancer receptor specificity. *Pro. Natl. Acad. Sci. USA*, **2010**, *107*(19), 8760-8765.

[10] Giljohann, D.A.; Seferos, D.S.; Daniel, W.L.; Massich, M.D.; Patel, P.C.; Mirkin, C.A. Gold nanoparticles for biology and medicine. *Angew. Chem. Int. Ed.*, **2010**, *49*(19), 3280-3294.

[11] Novoselov, K.S.; Geim, A.K.; Morozov, S.V.; Jiang, D.; Zhang, Y.; Dubonos, S.V.; Grigorieva, I.V.; Firsov, A.A. Electric Field Effect in Atomically Thin Carbon Films. *Science*, **2004**, *306*(5696), 666-669.

[12] Boehm, H.-P. Graphene—How a Laboratory Curiosity Suddenly Became Extremely Interesting. *Angew. Chem. Int. Ed.*, **2010**, *49*(49), 9332-9335.

[13] Matsumura, Y.; Maeda, H. A new concept for macromolecular therapeutics in cancer chemotherapy: mechanism of tumoritropic accumulation of proteins and the antitumor agent smancs. *Cancer Res.*, **1986**, *46*(12 Part 1), 6387-6392.

[14] Maeda H, M.Y. Tumoritropic and lymphotropic principles of macromolecular drugs. *Crit. Rev. Ther. Drug.*, **1989**, *6*(3), 193-210.

[15] Peer, D.; Karp, J.M.; Hong, S.; Farokhzad, O.C.; Margalit, R.; Langer, R. Nanocarriers as an emerging platform for cancer therapy. *Nat. Nanotechnol.*, **2007**, *2*(12), 751-760.

[16] Gu, F.X.; Karnik, R.; Wang, A.Z.; Alexis, F.; Levy-Nissenbaum, E.; Hong, S.; Langer, R.S.; Farokhzad, O.C. Targeted nanoparticles for cancer therapy. *Nano Today*, **2007**, *2*(3), 14-21.

[17] Wang, A.Z.; Gu, F.; Zhang, L.; Chan, J.M.; Radovic-Moreno, A.; Shaikh, M.R.; Farokhzad, O.C. Biofunctionalized targeted nanoparticles for therapeutic applications. *Expert Opin. Biol. Ther.*, **2008**, *8*(8), 1063-1070.

[18] Wang, X.; Yang, L.; Chen, Z.; Shin, D.M. Application of nanotechnology in cancer therapy and imaging. *CA Cancer J. Clin.*, **2008**, *58*(2), 97-110.

[19] Stohrer, M.; Boucher, Y.; Stangassinger, M.; Jain, R.K. Oncotic pressure in solid tumors is elevated. *Cancer Res.*, **2000**, *60*(15), 4251-4255.

[20] Qian, X.; Peng, X.-H.; Ansari, D.O.; Yin-Goen, Q.; Chen, G.Z.; Shin, D.M.; Yang, L.; Young, A.N.; Wang, M.D.; Nie, S. *In vivo* tumor targeting and spectroscopic detection with surface-enhanced raman nanoparticle tags. *Nat. Biotech.*, **2008**, *26*(1), 83-90.

[21] Frens, G. Controlled nucleation for regulation of particles-size in monodisperse gold suspensions. *Nature Phys. Sci.*, **1973**, *241*(105), 20-22.

[22] Brown, K.R.; Natan, M.J. Hydroxylamine seeding of colloidal Au nanoparticles in solution and on surfaces. *Langmuir*, **1998**, *14*(4), 726-728.

[23] Jana, N.R.; Gearheart, L.; Murphy, C.J. Seed-mediated growth approach for shape-controlled synthesis of spheroidal and rod-like gold nanoparticles using a surfactant template. *Adv. Mater.*, **2001**, *13*(18), 1389-1393.

[24] Jana, N.R.; Gearheart, L.; Murphy, C.J. Wet chemical synthesis of high aspect ratio cylindrical gold nanorods. *J. Phys. Chem. B*, **2001**, *105*(19), 4065-4067.

[25] Busbee, B.D.; Obare, S.O.; Murphy, C.J. An improved synthesis of high-aspect-ratio gold nanorods. *Adv. Mater.*, **2003**, *15*(5), 414-416.

[26] Sau, T.K.; Murphy, C.J. Room temperature, high-yield synthesis of multiple shapes of gold nanoparticles in aqueous solution. *J. Am. Chem. Soc.*, **2004**, *126*(28), 8648-8649.

[27] Chen, J.; McLellan, J.M.; Siekkinen, A.; Xiong, Y.; Li, Z.; Xia, Y. Facile synthesis of gold-silver nanocages with controllable pores on the surface. *J. Am. Chem. Soc.*, **2006**, *128*(46), 14776-14777.

[28] Skrabalak, S.E.; Au, L.; Li, X.; Xia, Y. Facile synthesis of Ag nanocubes and Au nanocages. *Nat. Protocols*, **2007**, *2*(9), 2182-2190.

[29] Skrabalak, S.E.; Chen, J.; Au, L.; Lu, X.; Li, X.; Xia, Y. Gold nanocages for biomedical applications. *Adv. Mater.*, **2007**, *19*(20), 3177-3184.

[30] Skrabalak, S.E.; Chen, J.; Sun, Y.; Lu, X.; Au, L.; Cobley, C.M.; Xia, Y. Gold nanocages: synthesis, properties, and applications. *Acc. Chem. Res.*, **2008**, *41*(12), 1587-1595.

[31] Subrata, K.; Sudipa, P.; Snigdhamayee, P.; Soumen, B.; Sujit, K.; Anjali, P.; Tarasankar, P. Anisotropic growth of gold clusters to gold nanocubes under UV irradiation. *Nanotechnology*, **2007**, *18*(7), 075712.

[32] Khanal, B.P.; Zubarev, E.R. Purification of high aspect ratio gold nanorods: complete removal of platelets. *J. Am. Chem. Soc.*, **2008**, *130*(38), 12634-12635.

[33] Kozlovskaya, V.; Kharlampieva, E.; Khanal, B.P.; Manna, P.; Zubarev, E.R.; Tsukruk, V.V. Ultrathin layer-by-layer hydrogels with incorporated gold nanorods as pH-sensitive optical materials. *Chem. Mater.*, **2008**, *20*(24), 7474-7485.

[34] Weiner, L.M.; Surana, R.; Wang, S. Monoclonal antibodies: versatile platforms for cancer immunotherapy. *Nat. Rev. Immunol.*, **2010**, *10*(5), 317-327.

[35] http://www.fda.gov/AboutFDA/CentersOffices/CDER/ucm093885.htm (Accessed November 12, 2010).

[36] Carter, P. Improving the efficacy of antibody-based cancer therapies. *Nat. Rev. Cancer*, **2001**, *1*(2), 118-129.

[37] Enback, J.; Laakkonen, P. Tumour-homing peptides: tools for targeting, imaging and destruction. *Biochem. Soc. Trans.*, **2007**, *035*(4), 780-783.

[38] Todd, O.P.; Matthew, A.P.; Brett, W.; Maroof, M.A.; Efrosini, K. Peptide- and aptamer-functionalized nanovectors for targeted delivery of therapeutics. *J. Biomech. Eng.*, **2009**, *131*(7), 074005.

[39] Li, J.; Ji, J.; Holmes, L.M.; Burgin, K.E.; Barton, L.B.; Yu, X.; Wagner, T.E.; Wei, Y. Fusion protein from RGD peptide and Fc fragment of mouse immunoglobulin G inhibits angiogenesis in tumor. *Cancer Gene Ther.*, **2004**, *11*(5), 363-370.

[40] Bies, C.; Lehr, C.M.; Woodley, J.F. Lectin-mediated drug targeting: history and applications. *Adv. Drug. Deliv. Rev.*, **2004**, *56*(4), 425-435.

[41] Davis, M.E.; Zuckerman, J.E.; Choi, C.H.J.; Seligson, D.; Tolcher, A.; Alabi, C.A.; Yen, Y.; Heidel, J.D.; Ribas, A. Evidence of RNAi in humans from systemically administered siRNA *via* targeted nanoparticles. *Nature*, **2010**, *464*(7291), 1067-1070.

[42] Kratz, F. Albumin as a drug carrier: Design of prodrugs, drug conjugates and nanoparticles. *J. Control. Release*, **2008**, *132*(3), 171-183.

[43] Zhou, J.; Rossi, J. Aptamer-targeted cell-specific RNA interference. *Silence*, **2010**, *1*(1), 4.

[44] Wang KY, M.S. Shea RG, Swaminathan S, Bolton PH. A DNA aptamer which binds to and inhibits thrombin exhibits a new structural motif for DNA. *Biochemistry*, **1993**, *32*(8), 1899-1904.

[45] Levy-Nissenbaum, E.; Radovic-Moreno, A.F.; Wang, A.Z.; Langer, R.; Farokhzad, O.C. Nanotechnology and aptamers: applications in drug delivery. *Trends Biotechnol.*, **2008**, *26*(8), 442-449.

[46] Ray, P.; White, R.R. Aptamers for targeted drug delivery. *Pharmaceuticals*, **2010**, *3*(6), 1761-1778.

[47] Keefe, A.D.; Pai, S.; Ellington, A. Aptamers as therapeutics. *Nat. Rev. Drug Discov.*, **2010**, *9*(7), 537-550.

[48] Asadishad, B.; Vossoughi, M.; Alemzadeh, I. Folate-receptor-targeted delivery of doxorubicin using polyethylene glycol-functionalized gold nanoparticles. *Ind. Eng. Chem. Res.*, **2010**, *49*(4), 1958-1963.

[49] Li, G.; Li, D.; Zhang, L.; Zhai, J.; Wang, E. One-step synthesis of folic acid protected gold nanoparticles and their receptor-mediated intracellular uptake. *Chem. Eur. J.*, **2009**, *15*(38), 9868-9873.

[50] Prabaharan, M.; Grailer, J.J.; Pilla, S.; Steeber, D.A.; Gong, S.Q. Gold nanoparticles with a monolayer of doxorubicin-conjugated amphiphilic block copolymer for tumor-targeted drug delivery. *Biomaterials*, **2009**, *30*(30), 6065-6075.

[51] Aslan, K.; Luhrs, C.C.; Perez-Luna, V.H. Controlled and reversible aggregation of biotinylated gold nanoparticles with streptavidin. *J. Phys. Chem. B*, **2004**, *108*(40), 15631-15639.

[52] Aslan, K.; Pérez-Luna, V. Nonradiative interactions between biotin-functionalized gold nanoparticles and fluorophore-labeled antibiotin. *Plasmonics*, **2006**, *1*(2), 111-119.

[53] Saul, J.M.; Annapragada, A.V.; Bellamkonda, R.V. A dual-ligand approach for enhancing targeting selectivity of therapeutic nanocarriers. *J. Control. Release*, **2006**, *114*(3), 277-287.

[54] Ying, X.; Wen, H.; Lu, W.L.; Du, J.; Guo, J.; Tian, W.; Men, Y.; Zhang, Y.; Li, R.J.; Yang, T.Y.; Shang, D.W.; Lou, J.N.; Zhang, L.R.; Zhang, Q. Dual-targeting daunorubicin liposomes improve the therapeutic efficacy of brain glioma in animals. *J. Control. Release*, **2010**, *141*(2), 183-192.

[55] Kluza, E.; van der Schaft, D.W.J.; Hautvast, P.A.I.; Mulder, W.J.M.; Mayo, K.H.; Griffioen, A.W.; Strijkers, G.J.; Nicolay, K. Synergistic targeting of alpha (v) beta (3) integrin and galectin-1 with heteromultivalent paramagnetic liposomes for combined MR imaging and treatment of angiogenesis. *Nano Lett.*, **2010**, *10*(1), 52-58.

[56] Li, X.; Zhou, H.Y.; Yang, L.; Du, G.; Pai-Panandiker, A.; Huang, X.F.; Yan, B. Enhancement of cell recognition *in vitro* by dual-ligand cancer targeting gold naoparticles. *Biomaterials*, **2011**, *doi:10.1016/j.biomaterials.2010.12.031*.

[57] Zhou, H.Y.; Jiao, P.F.; Yang, L.; Li, X.; Yan, B. Enhancing cell recognition by scrutinizing cell surfaces with a nanoparticle array. *J. Am. Chem. Soc.*, **2011**, *133*(4), 680-682.

[58] Han, G.; Ghosh, P.; De, M.; Rotello, V. Drug and gene delivery using gold nanoparticles. *Nanobiotechnol.*, **2007**, *3*(1), 40-45.

[59] Ghosh, P.; Han, G.; De, M.; Kim, C.K.; Rotello, V.M. Gold nanoparticles in delivery applications. *Adv. Drug. Deliv. Rev.*, **2008**, *60*(11), 1307-1315.

[60] Paciotti, G.F.; Myer, L.; Weinreich, D.; Goia, D.; Pavel, N.; McLaughlin, R.E.; Tamarkin, L. Colloidal gold: A novel nanoparticle vector for tumor directed drug delivery. *Drug Deliv.*, **2004**, *11*(3), 169-183.

[61] Paciotti, G.F.; Kingston, D.G.I.; Tamarkin, L. Colloidal gold nanoparticles: a novel nanoparticle platform for developing multifunctional tumor-targeted drug delivery vectors. *Drug Dev. Res.*, **2006**, *67*(1), 47-54.

[62] http://www.cytimmune.com/go.cfm?do=page.view&pid=19 (Accessed November 12, 2010).

[63] Libutti, S.K.; Paciotti, G.F.; Byrnes, A.A.; Alexander, H.R.; Gannon, W.E.; Walker, M.; Seidel, G.D.; Yuldasheva, N.; Tamarkin, L. Phase I and pharmacokinetic studies of CYT-6091, a novel PEGylated colloidal gold-rhTNF nanomedicine. *Clin. Cancer Res.*, **2010**, author manuscripts have been peer reviewed and accepted for publication but have not yet been edited.

[64] Libutti, S.K.; Paciotti, G.F.; Myer, L.; Haynes, R.; Gannon, W.; Walker, M.; Seidel, G.; Byrnes, A.; Yuldasheva, N.; Tamarkin, L. Results of a completed phase I clinical trial of CYT-6091: A pegylated colloidal gold-TNF nanomedicine. *J. Clin. Oncol. (Meeting Abstracts)*, **2009**, *27*(15S), 3586.

[65] Libutti, S.K.; Paciotti, G.F.; Myer, L.; Haynes, R.; Gannon, W.E. Jr.; Eugeni, M.; Seidel, G.; Shutack, Y.; Yuldasheva, N.; Tamarkin, L. Preliminary results of a phase I clinical trial of CYT-6091: A pegylated colloidal gold-TNF nanomedicine. *J. Clin. Oncol. (Meeting Abstracts)*, **2007**, *25*(18_suppl), 3603.

[66] http://clinicaltrials.gov/ct2/show/NCT00356980 (Accessed November 12, 2010).

[67] Chen, J.; Yang, M.; Zhang, Q.; Cho, E.C.; Cobley, C.M.; Kim, C.; Glaus, C.; Wang, L.V.; Welch, M.J.; Xia, Y. Gold nanocages: a novel class of multifunctional nanomaterials for theranostic applications. *Adv. Funct. Mater.*, **2010**, *20*(21), 3684-3694.

[68] Brun, E.; Duchambon, P.; Blouquit, Y.; Keller, G.; Sanche, L.; Sicard-Roselli, C. Gold nanoparticles enhance the X-ray-induced degradation of human centrin 2 protein. *Radiat. Phys. Chem.*, **2009**, *78*(3), 177-183.

[69] Popovtzer, R.; Agrawal, A.; Kotov, N.A.; Popovtzer, A.; Balter, J.; Carey, T.E.; Kopelman, R. Targeted gold nanoparticles enable molecular CT imaging of cancer. *Nano Lett.*, **2008**, *8*(12), 4593-4596.

[70] Hainfeld, J.F.; Dilmanian, F.A.; Slatkin, D.N.; Smilowitz, H.M. Radiotherapy enhancement with gold nanoparticles. *J. Pharm. Pharmacol.*, **2008**, *60*(8), 977-985.

[71] Kim, D.; Park, S.; Lee, J.H.; Jeong, Y.Y.; Jon, S. Antibiofouling polymer-coated gold nanoparticles as a contrast agent for *in vivo* X-ray computed tomography imaging. *J. Am. Chem. Soc.*, **2007**, *129*(24), 7661-7665.

[72] Guo, R.; Wang, H.; Peng, C.; Shen, M.; Pan, M.; Cao, X.; Zhang, G.; Shi, X. X-ray attenuation property of dendrimer-entrapped gold nanoparticles. *J. Phys. Chem. C*, **2009**, *114*(1), 50-56.

[73] Zhang, X.D.; Guo, M.L.; Wu, H.Y.; Sun, Y.M.; Ding, Y.Q.; Feng, X.; Zhang, L.A. Irradiation stability and cytotoxicity of gold nanoparticles for radiotherapy. *Int. J. Nanomed.*, **2009**, *4*, 165-173.

[74] Hainfeld, J.F.; Dilmanian, F.A.; Zhong, Z.; Slatkin, D.N.; Kalef-Ezra, J.A.; Smilowitz, H.M. Gold nanoparticles enhance the radiation therapy of a murine squamous cell carcinoma. *Phy. Med. Biol.*, **2010**, *55*(11), 3045-3059.

[75] Hainfeld, J.F.; Slatkin, D.N.; Smilowitz, H.M. The use of gold nanoparticles to enhance radiotherapy in mice. *Phy. Med. Biol.*, **2004**, *49*(18), N309-N315.

[76] Hainfeld, J.F.; Slatkin, D.N.; Smilowitz, H.M. The use of gold nanoparticles to enhance radiotherapy in mice. *Proc. Amer. Assoc. Cancer. Res.*, **2005**, *46*, 287.

[77] Pedro, R.N.; Thekke-Adiyat, T.; Goel, R.; Shenoi, M.; Slaton, J.; Schmechel, S.; Bischof, J.; Anderson, J.K. Use of tumor necrosis factor-alpha-coated gold nanoparticles to enhance radiofrequency ablation in a translational model of renal tumors. *Urology*, **2010**, *76*(2), 494-498.

[78] Sun, I.; Eun, D.; Na, J.; Lee, S.; Kim, I.; Youn, I.; Ko, C.; Kim, H.; Lim, D.; Choi, K.; Messersmith, P.; Park, T.; Kim, S.; Kwon, I.; Kim, K.; Ahn, C. Heparin-coated gold nanoparticles for liver-specific CT imaging. *Chem. Eur. J.*, **2009**, *15*(48), 13341-13347.

[79] Hainfeld, J.F.; Slatkin, D.N.; Focella, T.M.; Smilowitz, H.M. Gold nanoparticles: a new X-ray contrast agent. *Br. J. Radiol.*, **2006**, *79*(939), 248-253.

[80] Zhang, Z.; Ross, R.D.; Roeder, R.K. Preparation of functionalized gold nanoparticles as a targeted X-ray contrast agent for damaged bone tissue. *Nanoscale*, **2010**, *2*(4), 582-586.

[81] Kim, D.; Jeong, Y.Y.; Jon, S. A drug-loaded aptamer-gold nanoparticle bioconjugate for combined CT imaging and therapy of prostate cancer. *ACS Nano*, **2010**, *4*(7), 3689-3696.

[82] Ji, L.e.a. A novel functional CT contrast agent for molecular imaging of cancer. *Phy. Med. Biol.*, **2010**, *55*(15), 4389-4397.

[83] Katz, E.; Willner, I. Integrated nanoparticle–biomolecule hybrid systems: synthesis, properties, and applications. *Angew. Chem. Int. Ed.*, **2004**, *43*(45), 6042-6108.

[84] Nam, J.-M.; Thaxton, C.S.; Mirkin, C.A. Nanoparticle-based bio-bar codes for the ultrasensitive detection of proteins. *Science*, **2003**, *301*(5641), 1884-1886.

[85] Javier, D.J.; Nitin, N.; Levy, M.; Ellington, A.; Richards-Kortum, R. Aptamer-targeted gold nanoparticles as molecular-specific contrast agents for reflectance imaging. *Bioconjugate Chem.*, **2008**, *19*(6), 1309-1312.

[86] Liu, J.; Lu, Y. Preparation of aptamer-linked gold nanoparticle purple aggregates for colorimetric sensing of analytes. *Nat. Protocols*, **2006**, *1*(1), 246-252.

[87] Liu, X.; Dai, Q.; Austin, L.; Coutts, J.; Knowles, G.; Zou, J.; Chen, H.; Huo, Q. A one-step homogeneous immunoassay for cancer biomarker detection using gold nanoparticle probes coupled with dynamic light scattering. *J. Am. Chem. Soc.*, **2008**, *130*(9), 2780-2782.

[88] Thaxton, C.S.; Elghanian, R.; Thomas, A.D.; Stoeva, S.I.; Lee, J.-S.; Smith, N.D.; Schaeffer, A.J.; Klocker, H.; Horninger, W.; Bartsch, G.; Mirkin, C.A. Nanoparticle-based bio-barcode assay redefines "undetectable" PSA and biochemical recurrence after radical prostatectomy. *Pro. Natl. Acad. Sci. USA*, **2009**, *106*(44), 18437-18442.

[89] Bhattacharya, R.; Patra, C.R.; Earl, A.; Wang, S.; Katarya, A.; Lu, L.; Kizhakkedathu, J.N.; Yaszemski, M.J.; Greipp, P.R.; Mukhopadhyay, D.; Mukherjee, P. Attaching folic acid on gold nanoparticles using noncovalent interaction *via* different polyethylene glycol backbones and targeting of cancer cells. *Nanomed. Nanotechnol.*, **2007**, *3*(3), 224-238.

[90] Robert K DeLong, C.M.R. Yaneika Malcolm, Ashley Schaeffer, Tiffany Severs, Adam Wanekaya, Functionalized gold nanoparticles for the binding, stabilization, and delivery of therapeutic DNA, RNA, and other biological macromolecules. *Nanotechnology, Science and Applications*, **2010**, *3*, 53-63.

[91] Manuel Arruebo, M.V. and Africa González-Fernández, Antibody-conjugated nanoparticles for biomedical applications. *J. Nanomater.*, **2009**, 24 pages.

[92] Jadzinsky, P.D.; Calero, G.; Ackerson, C.J.; Bushnell, D.A.; Kornberg, R.D. Structure of a thiol monolayer-protected gold nanoparticle at 1.1 A resolution. *Science*, **2007**, *318*(5849), 430-433.

[93] Melancon, M.P.; Lu, W.; Yang, Z.; Zhang, R.; Cheng, Z.; Elliot, A.M.; Stafford, J.; Olson, T.; Zhang, J.Z.; Li, C. *In vitro* and *in vivo* targeting of hollow gold nanoshells directed at epidermal growth factor receptor for photothermal ablation therapy. *Mol. Cancer Ther.*, **2008**, *7*(6), 1730-1739.

[94] Hosta-Rigau, L.; Olmedo, I.; Arbiol, J.; Cruz, L.J.; Kogan, M.J.; Albericio, F. Multifunctionalized gold nanoparticles with peptides targeted to gastrin-releasing peptide receptor of a tumor cell line. *Bioconjugate Chem.*, **2010**, *21*(6), 1070-1078.

[95] Eck, W.; Craig, G.; Sigdel, A.; Ritter, G.; Old, L.J.; Tang, L.; Brennan, M.F.; Allen, P.J.; Mason, M.D. PEGylated gold nanoparticles conjugated to monoclonal F19 antibodies as targeted labeling agents for human pancreatic carcinoma tissue. *ACS Nano*, **2008**, *2*(11), 2263-2272.

[96] Yang, J.; Lee, J.; Kang, J.; Oh, S.J.; Ko, H.; Son, J.; Lee, K.; Suh, J.; Huh, Y.; Haam, S. Smart drug-loaded polymer gold nanoshells for systemic and localized therapy of human epithelial cancer. *Adv. Mater.*, **2009**, *21*(43), 4339-4342.

[97] Eghtedari, M.; Liopo, A.V.; Copland, J.A.; Oraevsky, A.A.; Motamedi, M. Engineering of hetero-functional gold nanorods for the *in vivo* molecular targeting of breast cancer cells. *Nano Lett.*, **2008**, *9*(1), 287-291.

[98] Park, C.; Youn, H.; Kim, H.; Noh, T.; Kook, Y.H.; Oh, E.T.; Park, H.J.; Kim, C. Cyclodextrin-covered gold nanoparticles for targeted delivery of an anti-cancer drug. *J. Mater. Chem.*, **2009**, *19*(16), 2310-2315.

[99] Kang, B.; Mackey, M.A.; El-Sayed, M.A. Nuclear targeting of gold nanoparticles in cancer cells induces DNA damage, causing cytokinesis arrest and apoptosis. *J. Am. Chem. Soc.*, **2010**, *132*(5), 1517-1519.

[100] Choi, C.H.J.; Alabi, C.A.; Webster, P.; Davis, M.E. Mechanism of active targeting in solid tumors with transferrin-containing gold nanoparticles. *Pro. Natl. Acad. Sci. USA*, **2010**, *107*(3), 1235-1240.

[101] Li, J.; Wang, L.; Liu, X.; Zhang, Z.; Guo, H.; Liu, W.; Tang, S. *In vitro* cancer cell imaging and therapy using transferrin-conjugated gold nanoparticles. *Cancer Lett.*, **2009**, *274*(2), 319-326.

[102] Wang, C.G.; Chen, J.; Talavage, T.; Irudayaraj, J. Gold nanorod/Fe3O4 nanoparticle "nano-pearl-necklaces" for simultaneous targeting, dual-mode imaging, and photothermal ablation of cancer cells. *Angew. Chem. Int. Ed.*, **2009**, *48*(15), 2759-2763.

[103] Wang, C.; Irudayaraj, J. Gold nanorod probes for the detection of multiple pathogens. *Small*, **2008**, *4*(12), 2204-2208.

[104] Wang, S.; Singh, A.K.; Senapati, D.; Neely, A.; Yu, H.; Ray, P.C. Rapid colorimetric identification and targeted photothermal lysis of salmonella bacteria by using bioconjugated oval-shaped gold nanoparticles. *Chem. Eur. J.*, **2010**, *16*(19), 5600-5606.

[105] Tong, L.; Wei, Q.; Wei, A.; Cheng, J. Gold nanorods as contrast agents for biological imaging: optical properties, surface conjugation and photothermal effects. *Photochem. Photobiol.*, **2009**, *85*(1), 21-32.

[106] Gole, A.; Murphy, C.J. Azide-derivatized gold nanorods: functional materials for "Click" Chemistry. *Langmuir*, **2007**, *24*(1), 266-272.

[107] Hainfeld, J.F.; Furuya, F.R. A 1.4-nm gold cluster covalently attached to antibodies improves immunolabeling. *J. Histochem. Cytochem.*, **1992**, *40*(2), 177-184.

[108] Kumar, S.; Aaron, J.; Sokolov, K. Directional conjugation of antibodies to nanoparticles for synthesis of multiplexed optical contrast agents with both delivery and targeting moieties. *Nat. Protocols*, **2008**, *3*(2), 314-320.

[109] Shi, M.; Wosnick, J.H.; Ho, K.; Keating, A.; Shoichet, M.S. Immuno-polymeric nanoparticles by Diels–Alder chemistry. *Angew. Chem. Int. Ed.*, **2007**, *46*(32), 6126-6131.

[110] Farokhzad, O.C.; Karp, J.M.; Langer, R. Nanoparticle-aptamer bioconjugates for cancer targeting. *Expert Opin. Drug Del.*, **2006**, *3*(3), 311-324.

[111] Huang, Y.; Lin, Y.; Lin, Z.; Chang, H. Aptamer-modified gold nanoparticles for targeting breast cancer cells through light scattering. *J. Nanopart. Res.*, **2009**, *11*(4), 775-783.

[112] Zhao, Q.; Lu, X.; Yuan, C.; Li, X.; Le, X. Aptamer-linked assay for thrombin using gold nanoparticle amplification and inductively coupled plasma-mass spectrometry detection. *Anal. Chem.*, **2009**, *81*(17), 7484-7489.

[113] Lee, R.J.; Low, P.S. In *Methods in Moleculer Medicine*. G.E. F.; C. D. Eds.; Humana Press Inc.: Totowa, NJ, **2000**; Vol. *25*, pp 69-75.

[114] Song, E.; Zhang, Z.; Luo, Q.; Lu, W.; Shi, Y.; Pang, D. Tumor cell targeting using folate-conjugated fluorescent quantum dots and receptor-mediated endocytosis. *Clin. Chem.*, **2009**, *55*(5), 955-963.

[115] Nie, Y.; Zhang, Z.; Li, L.; Luo, K.; Ding, H.; Gu, Z. Synthesis, characterization and transfection of a novel folate-targeted multipolymeric nanoparticles for gene delivery. *J. Mater. Sci.: Mater. Med.*, **2009**, *20*, 1849-1857

[116] Laurent, G.; Felidj, N.; Truong, S.L.; Aubard, J.; Levi, G.; Krenn, J.R.; Hohenau, A.; Leitner, A.; Aussenegg, F.R. Imaging surface plasmon of gold nanoparticle arrays by far-field raman scattering. *Nano Lett.*, **2004**, *5*(2), 253-258.

[117] Keren, S.; Zavaleta, C.; Cheng, Z.; de la Zerda, A.; Gheysens, O.; Gambhir, S.S. Noninvasive molecular imaging of small living subjects using Raman spectroscopy. *Pro. Natl. Acad. Sci. USA*, **2008**, *105*(15), 5844-5849.

[118] http://en.wikipedia.org/wiki/Photoacoustic_imaging_in_biomedicine (Accessed November 12, 2010).

[119] Mallidi, S.; Larson, T.; Tam, J.; Joshi, P.P.; Karpiouk, A.; Sokolov, K.; Emelianov, S. Multiwavelength photoacoustic imaging and plasmon resonance coupling of gold nanoparticles for selective detection of cancer. *Nano Lett.*, **2009**, *9*(8), 2825-2831.

[120] Yang, X.; Stein, E.W.; Ashkenazi, S.; Wang, L.V. Nanoparticles for photoacoustic imaging. *WIREs Nanomed. Nanobiotechnol.*, **2009**, *1*(4), 360-368.

[121] Agarwal, A.; Huang, S.W.; O'Donnell, M.; Day, K.C.; Day, M.; Kotov, N.; Ashkenazi, S. Targeted gold nanorod contrast agent for prostate cancer detection by photoacoustic imaging. *J. Appl. Phys.*, **2007**, *102*(6), 064701.

[122] Kim, J.W.; Galanzha, E.I.; Shashkov, E.V.; Moon, H.M.; Zharov, V.P. Golden carbon nanotubes as multimodal photoacoustic and photothermal high-contrast molecular agents. *Nat. Nanotechnol.*, **2009**, *4*(10), 688-694.

[123] Jin, Y.; Jia, C.; Huang, S.; O'Donnell, M.; Gao, X. Multifunctional nanoparticles as coupled contrast agents. *Nat. Commun.*, **2010**, *1*(4), 41.

[124] Kim, C.; Cho, E.C.; Chen, J.; Song, K.H.; Au, L.; Favazza, C.; Zhang, Q.; Cobley, C.M.; Gao, F.; Xia, Y.; Wang, L.V. *In vivo* molecular photoacoustic tomography of melanomas targeted by bioconjugated gold nanocages. *ACS Nano*, **2010**, *4*(8), 4559-4564.

[125] Song, K.H.; Kim, C.; Maslov, K.; Wang, L.V. Noninvasive *in vivo* spectroscopic nanorod-contrast photoacoustic mapping of sentinel lymph nodes. *Eur. J. Radiol.*, **2009**, *70*(2), 227-231.

[126] Xu, M.; Wang, L.V. Photoacoustic imaging in biomedicine. *Rev. Sci. Instrum.*, **2006**, *77*(4), 041101.

[127] Goel, R.; Shah, N.; Visaria, R.; Paciotti, G.F.; Bischof, J.C. Biodistribution of TNF-coated gold nanoparticles in an *in vivo* model system. *Nanomedicine*, **2009**, *4*(4), 401-410.

[128] Chen, J.; Glaus, C.; Laforest, R.; Zhang, Q.; Yang, M.; Gidding, M.; Welch, M.J.; Xia, Y. Gold nanocages as photothermal transducers for cancer treatment. *Small*, **2010**, *6*(7), 811-817.

[129] Li, Z.; Huang, P.; Zhang, X.; Lin, J.; Yang, S.; Liu, B.; Gao, F.; Xi, P.; Ren, Q.; Cui, D. RGD-conjugated dendrimer-modified gold nanorods for *in vivo* tumor targeting and photothermal therapy. *Mol. Pharm.*, **2009**, *7*(1), 94-104.

[130] Gibson, J.D.; Khanal, B.P.; Zubarev, E.R. Paclitaxel-functionalized gold nanoparticles. *J. Am. Chem. Soc.*, **2007**, *129*, 11653-11661.

[131] Hwu, J.R.; Lin, Y.S.; Josephrajan, T.; Hsu, M.H.; Cheng, F.Y.; Yeh, C.S.; Su, W.C.; Shieh, D.B. Targeted paclitaxel by conjugation to iron oxide and gold nanoparticles. *J. Am. Chem. Soc.*, **2009**, *131*(1), 66-68.

[132] Aryal, S.; Grailer, J.J.; Pilla, S.; Steeber, D.A.; Gong, S.Q. Doxorubicin conjugated gold nanoparticles as water-soluble and pH-responsive anticancer drug nanocarriers. *J. Mater. Chem.*, **2009**, *19*(42), 7879-7884.

[133] Brown, S.D.; Nativo, P.; Smith, J.A.; Stirling, D.; Edwards, P.R.; Venugopal, B.; Flint, D.J.; Plumb, J.A.; Graham, D.; Wheate, N.J. Gold nanoparticles for the improved anticancer drug delivery of the active component of oxaliplatin. *J. Am. Chem. Soc.*, **2010**, *132*(13), 4678-4684.

[134] Dhar, S.; Daniel, W.L.; Giljohann, D.A.; Mirkin, C.A.; Lippard, S.J. Polyvalent oligonucleotide gold nanoparticle conjugates as delivery vehicles for platinum (IV) warheads. *J. Am. Chem. Soc.*, **2009**, *131*(41), 14652-14653.

[135] Sies, H. Glutathione and its role in cellular functions. *Free Radical Biol. Med.*, **1999**, *27*(9-10), 916-921.

[136] Hong, R.; Han, G.; Fernandez, J.M.; Kim, B.J.; Forbes, N.S.; Rotello, V.M. Glutathione-mediated delivery and release using monolayer protected nanoparticle carriers. *J. Am. Chem. Soc.*, **2006**, *128*(4), 1078-1079.

[137] Kim, C.K.; Ghosh, P.; Pagliuca, C.; Zhu, Z.J.; Menichetti, S.; Rotello, V.M. Entrapment of hydrophobic drugs in nanoparticle monolayers with efficient release into cancer cells. *J. Am. Chem. Soc.*, **2009**, *131*(4), 1360-1361.

[138] Agasti, S.S.; Chompoosor, A.; You, C.C.; Ghosh, P.; Kim, C.K.; Rotello, V.M. Photoregulated release of caged anticancer drugs from gold nanoparticles. *J. Am. Chem. Soc.*, **2009**, *131*(16), 5728-5729.

[139] Ipe, B.I.; Mahima, S.; Thomas, K.G. Light-induced modulation of self-assembly on spiropyran-capped gold nanoparticles: A potential system for the controlled release of amino acid derivatives. *J. Am. Chem. Soc.*, **2003**, *125*(24), 7174-7175.

[140] Nakanishi, J.; Nakayama, H.; Shimizu, T.; Ishida, H.; Kikuchi, Y.; Yamaguchi, K.; Horiike, Y. Light-regulated activation of cellular signaling by gold nanoparticles that capture and release amines. *J. Am. Chem. Soc.*, **2009**, *131*(11), 3822-3823.

[141] Vivero-Escoto, J.L.; Slowing, II; Wu, C.W.; Lin, V.S.Y. Photoinduced intracellular controlled release drug delivery in human cells by gold-capped mesoporous silica nanosphere. *J. Am. Chem. Soc.*, **2009**, *131*(10), 3462-3463.

[142] Jiang, W.; KimBetty, Y.S.; Rutka, J.T.; ChanWarren, C.W. Nanoparticle-mediated cellular response is size-dependent. *Nat. Nanotechnol.*, **2008**, *3*(3), 145-150.

[143] Singh, Y.; Palombo, M.; Sinko, P.J. Recent trends in targeted anticancer prodrug and conjugate design. *Curr. Med. Chem.*, **2008**, *15*(18), 1802-1826.

[144] Pissuwan, D.; Cortie, C.H.; Valenzuela, S.M.; Cortie, M.B. Gold nanosphere-antibody conjugates for hyperthermal therapeutic applications. *Gold Bull.*, **2007**, *40*(2), 121-129.

[145] Huang, X.; Qian, W.; El-Sayed, I.H.; El-Sayed, M.A. The potential use of the enhanced nonlinear properties of gold nanospheres in photothermal cancer therapy. *Lasers Surg. Med.*, **2007**, *39*, 747-753.

[146] Lu, W.; Xiong, C.Y.; Zhang, G.D.; Huang, Q.; Zhang, R.; Zhang, J.Z.; Li, C. Targeted photothermal ablation of murine melanomas with melanocyte-stimulating hormone analog-conjugated hollow gold nanospheres. *Clin. Cancer Res.*, **2009**, *15*(3), 876-886.

[147] Skala, M.C.; Crow, M.J.; Wax, A.; Izatt, J.A. Photothermal optical coherence tomography of epidermal growth factor receptor in live cells using immunotargeted gold nanospheres. *Nano Lett.*, **2008**, *8*(10), 3461-3467.

[148] Wang, S.T.; Chen, K.J.; Wu, T.H.; Wang, H.; Lin, W.Y.; Ohashi, M.; Chiou, P.Y.; Tseng, H.R. Photothermal effects of supramolecularly assembled gold nanoparticles for the targeted treatment of cancer cells. *Angew. Chem. Int. Ed.*, **2010**, *49*(22), 3777-3781.

[149] Huang, X.H.; El-Sayed, I.H.; Qian, W.; El-Sayed, M.A. Cancer cell imaging and photothermal therapy in the near-infrared region by using gold nanorods. *J. Am. Chem. Soc.*, **2006**, *128*(6), 2115-2120.

[150] Norman, R.S.; Stone, J.W.; Gole, A.; Murphy, C.J.; Sabo-Attwood, T.L. Targeted photothermal lysis of the pathogenic bacteria, pseudomonas aeruginosa, with gold nanorods. *Nano Lett.*, **2008**, *8*(1), 302-306.

[151] Huff, T.B.; Tong, L.; Zhao, Y.; Hansen, M.N.; Cheng, J.X.; Wei, A. Hyperthermic effects of gold nanorods on tumor cells. *Nanomedicine*, **2007**, *2*(1), 125-132.

[152] Tong, L.; Zhao, Y.; Huff, T.B.; Hansen, M.N.; Wei, A.; Cheng, J.X. Gold nanorods mediate tumor cell death by compromising membrane integrity. *Adv. Mater.*, **2007**, *19*, 3136-3141.

[153] Von Maltzahn, G.; Park, J.H.; Agrawal, A.; Bandaru, N.K.; Das, S.K.; Sailor, M.J.; Bhatia, S.N. Computationally guided photothermal tumor therapy using long-circulating gold nanorod antennas. *Cancer Res.*, **2009**, *69*(9), 3892-3900.

[154] Au, L.; Zheng, D.S.; Zhou, F.; Li, Z.Y.; Li, X.D.; Xia, Y.N. A quantitative study on the photothermal effect of immuno gold nanocages targeted to breast cancer cells. *ACS Nano*, **2008**, *2*(8), 1645-1652.

[155] Chen, J.Y.; Wang, D.L.; Xi, J.F.; Au, L.; Siekkinen, A.; Warsen, A.; Li, Z.Y.; Zhang, H.; Xia, Y.N.; Li, X.D. Immuno gold nanocages with tailored optical properties for targeted photothermal destruction of cancer cells. *Nano Lett.*, **2007**, *7*, 1318-1322.

[156] Cobley, C.M.; Au, L.; Chen, J.Y.; Xia, Y.N. Targeting gold nanocages to cancer cells for photothermal destruction and drug delivery. *Expert Opin. Drug Del.*, **2010**, *7*(5), 577-587.

[157] Hu, M.; Petrova, H.; Chen, J.Y.; McLellan, J.M.; Siekkinen, A.R.; Marquez, M.; Li, X.D.; Xia, Y.N.; Hartland, G.V. Ultrafast laser studies of the photothermal properties of gold nanocages. *J. Phys. Chem. B*, **2006**, *110*(4), 1520-1524.

[158] Rycenga, M.; Wang, Z.P.; Gordon, E.; Cobley, C.M.; Schwartz, A.G.; Lo, C.S.; Xia, Y.N. Probing the photothermal effect of gold-based nanocages with surface-enhanced raman scattering (SERS). *Angew. Chem. Int. Ed.*, **2009**, *48*(52), 9924-9927.

[159] Nam, J.; Won, N.; Jin, H.; Chung, H.; Kim, S. pH-Induced aggregation of gold nanoparticles for photothermal cancer therapy. *J. Am. Chem. Soc.*, **2009**, *131*(38), 13639-13645.

[160] Cheng, Y.; Samia, A.C.; Meyers, J.D.; Panagopoulos, I.; Fei, B.W.; Burda, C. Highly efficient drug delivery with gold nanoparticle vectors for *in vivo* photodynamic therapy of cancer. *J. Am. Chem. Soc.*, **2008**, *130*(32), 10643-10647.

[161] Matsudaira, H.; Ueno, A.M.; Furuno, I. Iodine contrast-medium sensitizes sultured mammalian-cells to X-rays but not to gamma-rays. *Radiat. Res.*, **1980**, *84*(1), 144-148.

[162] Hainfeld, J.F.; *et al*. The use of gold nanoparticles to enhance radiotherapy in mice. *Phy. Med. Biol.*, **2004**, *49*(18), N309.

[163] Cho, S.H. Estimation of tumour dose enhancement due to gold nanoparticles during typical radiation treatments: a preliminary Monte Carlo study. *Phy. Med. Biol.*, **2005**, *50*(15), N163.

[164] Kong, T.; Zeng, J.; Wang, X.; Yang, X.; Yang, J.; McQuarrie, S.; McEwan, A.; Roa, W.; Chen, J.; Xing, J.Z. Enhancement of Radiation Cytotoxicity in Breast-Cancer Cells by Localized Attachment of Gold Nanoparticles. *Small*, **2008**, *4*(9), 1537-1543.

Received: January 08, 2011 **Revised: April 05, 2011** **Accepted: April 06, 2011**

[165] Liu, C.-J.; *et al*. Enhanced x-ray irradiation-induced cancer cell damage by gold nanoparticles treated by a new synthesis method of polyethylene glycol modification. *Nanotechnology*, **2008**, *19*(29), 295104.

[166] Wan Nordiana, R.; Nour, B.; Trevor, A.; Cheng Fa, H.; Price, J.; Christopher, W.; Robert, D.; Moshi, G. Enhancement of radiation effects by gold nanoparticles for superficial radiation therapy. *Nanomed.-Nanotechnol. Biol. Med.*, **2009**, *5*(2), 136-142.

[167] Hainfeld, J.F.; *et al*. Gold nanoparticles enhance the radiation therapy of a murine squamous cell carcinoma. *Phy. Med. Biol.*, **2010**, *55*(11), 3045.

[168] Chithrani, D.B.; Jelveh, S.; Jalali, F.; van Prooijen, M.; Allen, C.; Bristow, R.G.; Hill, R.P.; Jaffray, D.A. Gold nanoparticles as radiation sensitizers in cancer therapy. *Radiat. Res.*, **2010**, *173*(6), 719-728.

[169] Cai, W.; Chen, X. Nanoplatforms for targeted molecular imaging in living subjects. *Small*, **2007**, *3*(11), 1840-1854.

[170] Torigian, D.A.; Huang, S.S.; Houseni, M.; Alavi, A. Functional imaging of cancer with emphasis on molecular techniques. *CA Cancer J. Clin.*, **2007**, *57*(4), 206-224.

[171] Rusinek, H.; Naidich, D.P.; McGuinness, G.; Leitman, B.S.; McCauley, D.I.; Krinsky, G.A.; Clayton, K.; Cohen, H. Pulmonary nodule detection: Low-dose versus conventional CT. *Radiology*, **1998**, *209*(1), 243-249.